

Exploiting the links between ground-state correlations and independent-fermion entropy in the Hubbard model

T. S. Müller, W. Töws, and G. M. Pastor

Institut für Theoretische Physik, Universität Kassel, Heinrich Plett Strasse 40, 34132 Kassel, Germany



(Received 23 September 2016; revised manuscript received 9 May 2018; published 26 July 2018)

The ground-state properties of the half-filled Hubbard model are investigated in the framework of lattice density functional theory. The single-particle density matrix $\gamma_{ij\sigma}$ is regarded as the central variable of the many-body problem, where i and j refer to the lattice sites and σ to the spin. The interaction-energy functional $W[\gamma_{ij\sigma}]$ is calculated exactly for representative finite periodic systems by performing exact Lanczos diagonalizations. The relationship between $W[\gamma_{ij\sigma}]$ and the entropy $S[\eta_{k\sigma}]$ of independent fermions with natural-orbital occupations $\eta_{k\sigma}$ is analyzed. A simple approximation to the interaction energy of the half-filled Hubbard model is proposed, which takes the form $W = W(S[\eta_{k\sigma}])$. Using this functional we derive the ground-state energy, kinetic energy, average number of double occupations, charge distribution, magnetic susceptibility, and field-induced spin polarization in one-, two-, and three-dimensional periodic lattices. The limit of infinite dimensions is also explored. The accuracy of the method is assessed by comparison with available exact numerical or analytical results. Goals, limitations, and possible extensions of the domain of applicability of the functional are discussed.

DOI: [10.1103/PhysRevB.98.045135](https://doi.org/10.1103/PhysRevB.98.045135)

I. INTRODUCTION

The quantum many-body problem has always been one of the most important challenges in condensed-matter physics. From a first-principles perspective, the most significant progress over the past decades has been achieved in the framework of density functional theory (DFT). The density functional methodology builds on the seminal theorem of Hohenberg and Kohn [1], which states that the ground-state properties of electrons in an arbitrary external potential can be regarded as functionals of the electronic density $n(\mathbf{r})$. The underlying one-to-one mapping between the ground state and $n(\mathbf{r})$ allows us in principle to avoid the calculation of the ground-state wave function $|\psi\rangle$. Thus, $n(\mathbf{r})$ takes the role of the fundamental variable of the many-body problem.

Most practical applications of DFT are performed within the Kohn-Sham scheme, which reduces the interacting many-particle problem to a set of self-consistent single-particle equations [2]. A central concept in this context is the functional $F[n(\mathbf{r})] = T[n(\mathbf{r})] + W[n(\mathbf{r})]$ giving the optimal sum of the kinetic energy $T[n(\mathbf{r})]$ and the interaction energy $W[n(\mathbf{r})]$ of an electronic system having an arbitrary physical $n(\mathbf{r})$. Although formally exact, the applications of DFT are hindered by the fact that the explicit form of $F[n(\mathbf{r})]$ remains unknown. Consequently, the actual calculations must resort to some approximation to $F[n(\mathbf{r})]$, among which the local spin-density approximation (LSDA) [2,3], the generalized-gradient approximations (GGAs) [4–6], and the so-called hybrid functionals [7–9] are the most widespread at present. More recently, related methods based on the single-particle density matrix $\gamma(\mathbf{r}, \mathbf{r}')$ have also been developed [10–22].

Hohenberg-Kohn-Sham's theory has demonstrated its predictive power in countless applications throughout the most large variety of fields. However, there are still several open problems, where the conventional exchange and correlation

functionals perform poorly. This applies in particular to strong electron-correlation effects, for example, the dissociation of closed-shell molecules [23], the physics of heavy-fermion materials [24], high-temperature superconductivity [25], and Mott insulators [26–28]. Finding an accurate DFT description of these phenomena remains a serious challenge [29–34]. In order to understand the properties of these systems, several many-body lattice Hamiltonians have been developed, which focus on the most relevant dynamics of the valence electrons. Motivated at the origin by the description of molecular bonding [35,36], magnetic impurities in metals [37], and itinerant electrons in narrow bands [38–40], the theory of many-body models has grown to a high level of sophistication, not only from a methodological perspective, but also concerning the physical effects that are taken into account in the modelization. In this way, subtle phenomena such as valence and spin fluctuations, separation of charge and spin degrees of freedom, superconductivity, correlation-induced localization, etc., have been revealed [25,41,42]. Despite these achievements, and although the electron dynamics is simplified with respect to the full first-principles problem, deriving the properties of these models remains a very difficult task. Exact analytical results are rare [43–47], and accurate numerical solutions are either inaccessible or very demanding [26,48–51]. Consequently, developing theoretical methods capable of describing the physics of many-body lattice Hamiltonians is a subject of considerable interest.

In past years, a number of studies of electron correlations have been performed by applying the concepts of DFT to lattice models [52–65,65–69]. Indeed, taking into account the universality of DFT, and its demonstrated efficiency in complex *ab initio* calculations, it is reasonable to expect that DFT, with an appropriate ansatz for the kinetic- and interaction-energy functionals, should be a most valuable approach to correlated lattice models. Early studies have addressed the

band-gap problem in semiconductors [52–54] and the role of the off-diagonal elements of the density matrix in order to describe strong electron correlations [55]. Density-matrix energy functionals have been proposed and applied to the Anderson model [56]. Moreover, local approximations have been derived based on the Bethe-ansatz exact solution of the one-dimensional Hubbard model [57], and time-dependent approaches have been developed [58]. Particularly relevant in the context of this paper is the lattice density functional theory (LDFT) formulated in Refs. [59,60], which considers the single-particle density matrix $\gamma_{ij\sigma}$ as the central variable of the many-body problem.

The LDFT approach has been successfully applied to a variety of physical situations involving strong electron correlations, for example, the single-impurity Anderson model [63–65], the Hubbard model with homogeneous and inhomogeneous local potentials, dimerized chains, attractive pairing interactions, and inhomogeneous local repulsions [60–62,65–69]. The basic idea behind the available functionals is to adopt a real-space perspective and to take advantage of the scaling properties of W as a function of the bond order $\gamma_{12\sigma}$, which measures the degree of charge fluctuations between nearest neighbors (NNs). The actual dependence of W on $\gamma_{12\sigma}$ can then be inferred from a simple reference system, for instance, the Hubbard dimer. In its simplest version, this approach gives access only to the diagonal and NN elements of the density matrix. Models having interatomic hoppings beyond NNs cannot usually be treated in this framework, although an extension has been recently proposed, which overcomes this limitation [69]. Therefore, the domain of applicability of the functionals proposed so far for the Hubbard model and the properties that can be derived from them are somewhat limited. Moreover, describing the dependence of W on the complete density matrix γ is necessary in order to be able to take full advantage of the universality of LDFT. In fact, only in this case the interaction-energy functional is completely independent from the topology, dimensionality and structure of the system. A more flexible formulation would also allow us to predict the distance dependence of $\gamma_{ij\sigma}$, even if the actual hybridizations are short ranged, as usually found in narrow-band systems. This would be interesting in order to analyze how electron localization develops in real space with increasing Coulomb-repulsion strength, which is also relevant for transport properties. Finally, knowing all nonvanishing $\gamma_{ij\sigma}$ would allow us to determine the average occupation numbers of the translational-invariant Bloch states along the crossover from weak to strong correlations. It is the goal of this paper to develop an interaction-energy functional $W[\gamma]$ for the Hubbard model by adopting a delocalized \mathbf{k} -space perspective. To this aim, we focus on homogeneous periodic systems and investigate the dependence of W on the eigenvalues $\eta_{\mathbf{k}\sigma}$ of γ_{σ} , which define the average occupation of the natural orbitals and thus represent the spin-polarized electronic density in \mathbf{k} space. A simple energy functional $E[\eta_{\mathbf{k}\sigma}]$ is proposed for the half-filled Hubbard model, which exploits certain analogies between ground-state electron correlations and the entropy of independent fermions having the occupation-number distribution $\eta_{\mathbf{k}\sigma}$. This functional is subsequently applied in the framework of LDFT to one-, two-, and three-dimensional lattices.

The remainder of the paper is organized as follows. In Sec. II the fundamental concepts of LDFT are briefly recalled, giving emphasis to its application to periodic systems. In Sec. III the relationship between independent-fermion entropy S and degree of electron correlations in the half-filled Hubbard model is discussed. This leads to a simple ansatz for the interaction-energy functional $W[\gamma]$, whose properties are analyzed in the limits of weak and strong correlations. Results for finite and infinite periodic lattices are presented and discussed in Sec. IV. The accuracy of the proposed approximation to W is assessed by comparison with exact results whenever possible. Finally, Sec. V summarizes our main conclusions and points out some possible future extensions.

II. DENSITY FUNCTIONAL THEORY ON A LATTICE

A. General formulation

Given a discrete basis set of single-particle orbitals $\{\phi_i(\mathbf{r})\}$, a nonrelativistic many-electron system is described by the Hamiltonian

$$\hat{H} = \hat{T} + \hat{W} = \sum_{ij\sigma} t_{ij} \hat{c}_{i\sigma}^\dagger \hat{c}_{j\sigma} + \sum_{ijkl} W_{ijkl} \hat{c}_{i\sigma}^\dagger \hat{c}_{j\sigma}^\dagger \hat{c}_{l\sigma'} \hat{c}_{k\sigma}, \quad (1)$$

where $\hat{c}_{i\sigma}^\dagger$ ($\hat{c}_{i\sigma}$) creates (annihilates) a particle with spin σ at the orbital $\phi_i(\mathbf{r})$. The index i denotes the lattice site as well as the different local orbitals. The parameters t_{ij} are single-particle matrix elements, where $\varepsilon_i = t_{ii}$ refers to the energy levels and t_{ij} for $i \neq j$ to the hopping integrals. The interaction term is characterized by the Coulomb integrals W_{ijkl} [25]. Once a basis set $\{\phi_i(\mathbf{r})\}$ is adopted, only the single-particle matrix elements t_{ij} depend on the external potential $v(\mathbf{r})$ acting on the electrons. Therefore, in the spirit of DFT, they define the actual problem under study. From the perspective of lattice models the hopping matrix t_{ij} specifies the topology and dimensionality of the lattice, as well as the range of the single-particle hybridizations.

The Hohenberg-Kohn (HK) theorem [1] states that in the absence of degeneracies the ground-state electron density $n(\mathbf{r})$ defines unambiguously the ground-state wave function $|\psi\rangle$ of any electronic system subject to a local potential $v(\mathbf{r})$. It is therefore interesting to consider the density operator $\hat{n}(\mathbf{r}) = \sum_{\sigma} \hat{\psi}_{\sigma}^\dagger(\mathbf{r}) \hat{\psi}_{\sigma}(\mathbf{r})$ by expressing the field operators $\hat{\psi}_{\sigma}^\dagger(\mathbf{r})$ and $\hat{\psi}_{\sigma}(\mathbf{r})$ in terms of the basis functions $\phi_i(\mathbf{r})$ and the corresponding creation and annihilation operators. Since

$$\hat{n}(\mathbf{r}) = \sum_{ij\sigma} \phi_i^*(\mathbf{r}) \phi_j(\mathbf{r}) \hat{c}_{i\sigma}^\dagger \hat{c}_{j\sigma}, \quad (2)$$

the particle density $n(\mathbf{r})$ in any state $|\psi\rangle$ is given by

$$n(\mathbf{r}) = \langle \psi | \hat{n}(\mathbf{r}) | \psi \rangle = \sum_{ij\sigma} \gamma_{ij\sigma} \phi_i^*(\mathbf{r}) \phi_j(\mathbf{r}), \quad (3)$$

where

$$\gamma_{ij\sigma} = \langle \psi | \hat{c}_{i\sigma}^\dagger \hat{c}_{j\sigma} | \psi \rangle \quad (4)$$

denotes the elements of the single-particle density matrix (SPDM). Equation (3) shows that γ defines $n(\mathbf{r})$, the fundamental variable of DFT, in any many-body state $|\psi\rangle$. Notice, moreover, that all matrix elements $\gamma_{ij\sigma}$ are required in order to

determine $n(\mathbf{r})$ completely, once the basis set $\{\phi_i(\mathbf{r})\}$ is fixed. As we shall see, the importance of the off-diagonal elements of γ is a consequence of the nonlocality of the hopping integrals t_{ij} . Furthermore, an independent lattice version of the HK theorem has been formulated, which demonstrates the existence of a unique mapping between nondegenerate ground states $|\psi_0\rangle$ and the corresponding density matrix γ^0 [63]. In this work, a universal formulation of density functional theory is aimed, i.e., one which applies to arbitrary lattice structures, dimensions, and hopping integrals t_{ij} . Therefore, it is necessary to consider the full SPDM γ as the fundamental variable of the many-body problem. A similar situation is found in the continuum when nonlocal pseudopotentials are considered (see Ref. [10]). Notice, however, that alternative density functional descriptions of many-body lattice models have been proposed, which are based solely on the diagonal elements $\gamma_{i\sigma} = n_{i\sigma}$ of the SPDM, i.e., on the density or site occupation numbers $n_{i\sigma}$ [52–58]. While this approach is rigorously valid, the associated interaction-energy functionals $W[n_{i\sigma}]$ depend on the considered lattice structure and hopping integrals t_{ij} . Let us finally mention that interaction-energy functionals of the single-particle density matrix $\gamma(\mathbf{r}, \mathbf{r}')$ have also been proposed in order to study problems with local potentials $v(\mathbf{r})$, even though this is not required by the Hohenberg-Kohn theorem [11–22].

The ground-state energy functional can be written as

$$E[\gamma] = T[\gamma] + W[\gamma], \quad (5)$$

where

$$T[\gamma] = \sum_{ij\sigma} t_{ij} \gamma_{ij\sigma} \quad (6)$$

denotes the single-particle contribution representing the kinetic and potential energy of the electrons in the lattice. The second term in (5) is the interaction-energy functional

$$W[\gamma] = \min_{|\psi\rangle \rightarrow \gamma} \left[\sum_{\substack{ijkl \\ \sigma\sigma'}} W_{ijkl} \langle \psi | \hat{c}_{i\sigma}^\dagger \hat{c}_{j\sigma'}^\dagger \hat{c}_{l\sigma'} \hat{c}_{k\sigma} | \psi \rangle \right], \quad (7)$$

which represents the minimum interaction energy among all N -particle states $|\psi\rangle$ that yield the given γ according to Eq. (4) [59,70]. Notice that, in contrast to $T[\gamma]$, the explicit form of the functional $W[\gamma]$ is not known in general. Therefore, the main challenge in LDFT is to find good approximations to W .

Before formulating a minimization scheme for the energy E , it is useful to discuss the domain of definition of W as a functional of γ . Equation (7) implies a minimization over the set of all $|\psi\rangle$ which yield the density matrix $\gamma_{ij\sigma}$. In order that this set is not empty, and that the definition of $W[\gamma]$ makes sense, one needs to restrict the domain of definition of $W[\gamma]$ to pure-state N -representable γ , i.e., to the density matrices that can be obtained from Eq. (4) for some many-body state $|\psi\rangle$. This set includes, of course, the density matrix γ^0 corresponding to the ground state $|\psi_0\rangle$, from which the energy E_0 and the expectation values $\mathcal{O}[\gamma^0] = \langle \psi_0 | \hat{\mathcal{O}} | \psi_0 \rangle$ of other observables \mathcal{O} are obtained. It is well known that all SPDMs are necessarily diagonalizable with eigenvalues $\eta_{k\sigma}$ satisfying $0 \leq \eta_{k\sigma} \leq 1$. However, a sufficient condition characterizing pure state N -representable SPDMs is not known at present.

And yet such a criterion exists for the larger set of ensemble- N -representable density matrices $\gamma_{ij\sigma} = \text{Tr}\{\hat{\rho} \hat{c}_{i\sigma}^\dagger \hat{c}_{j\sigma}\}$, which are derived from mixed-state density operators $\hat{\rho}$. In this case the above-mentioned necessary condition is also sufficient. For this reason, we extend the domain of definition for the functionals (5)–(7) to the larger set of ensemble-representable density matrices. In this case the minimization in Eq. (7) should run over all density operators $\hat{\rho}$ yielding the given γ . This should have no consequences in practice since for integer N the minimum of the energy functional (5) over the set of ensemble-representable density matrices corresponds to a pure-state N -representable $\gamma_{ij\sigma}$, namely, the density matrix $\gamma_{ij\sigma}^0$ of the ground state. Therefore, extending the domain of definition should not change the physical results. Notice, however, that the previous considerations need not strictly hold when approximations to $W[\gamma]$ are involved.

In order to obtain the equations giving the ground-state properties we express

$$\gamma_{ij\sigma} = \sum_k u_{ik\sigma} \eta_{k\sigma} u_{jk\sigma}^* \quad (8)$$

in terms of its eigenvectors or natural orbitals $u_{ik\sigma}$ and of its eigenvalues or orbital occupations $\eta_{k\sigma}$. The stationary condition on the energy functional (5) with respect to variations of $u_{ik\sigma}^*$ and $\eta_{k\sigma}$ under the constraints

$$\sum_k \eta_{k\sigma} = N_\sigma \quad (9)$$

on the number of spin- σ electrons N_σ , and

$$\sum_i |u_{ik\sigma}|^2 = 1 \quad (10)$$

on the normalization of the natural orbitals, yields the coupled equations

$$\sum_i \frac{\partial E[\gamma]}{\partial \gamma_{ij\sigma}} u_{ik\sigma} = \lambda_{k\sigma} u_{jk\sigma} \quad (11)$$

and

$$\frac{\partial E[\gamma]}{\partial \eta_{k\sigma}} = \mu_{k\sigma}. \quad (12)$$

These equations can in general be solved by means of the double-loop iterative procedure proposed in Ref. [69]. In this scheme, the orbital occupations $\eta_{k\sigma}$ are first optimized keeping the current ansatz for the natural orbitals $u_{ik\sigma}$ fixed. The thus obtained $\gamma_{ij\sigma}$ allows one to calculate $\partial E / \partial \gamma_{ij\sigma}$ and thus the new eigenvectors $u_{ik\sigma}$ according to Eq. (11). These represent the natural orbitals to be used in the optimization of $\eta_{k\sigma}$ in the subsequent iteration, until convergence is achieved. Nevertheless, in this study, no numerical iterative procedure is actually necessary since an exact analytic solution of the self-consistent equations (11) and (12) can be obtained for the proposed functional dependence of the interaction energy $W[\eta_{k\sigma}]$.

B. Periodic systems

For the purpose of deriving an approximation to the interaction-energy functional we focus on homogeneous, periodic single-band systems. In this case, due to the translational

symmetry, the ground-state SPDM depends only on the vector connecting the lattice sites \mathbf{R}_i and \mathbf{R}_j , i.e., $\gamma_{ij\sigma} = \gamma_\sigma(\mathbf{R}_i - \mathbf{R}_j)$ and in particular $\gamma_{ii\sigma} = N_\sigma/N_a$ is independent of i . Applying the Bloch theorem to γ_σ one obtains the eigenvectors

$$u_{ik\sigma} = \frac{1}{\sqrt{N_a}} e^{-ik \cdot \mathbf{R}_i}, \quad (13)$$

which are classified by the wave vectors \mathbf{k} in the first Brillouin zone (BZ). Substituting Eq. (13) into Eq. (8), one finds

$$\gamma_{ij\sigma} = \frac{1}{N_a} \sum_{\mathbf{k} \in \text{BZ}} \eta_{k\sigma} e^{-ik \cdot (\mathbf{R}_i - \mathbf{R}_j)}, \quad (14)$$

which is characterized by the occupation numbers $\eta_{k\sigma}$. Consequently for periodic systems, the occupation numbers $\eta_{k\sigma}$ can be regarded as the fundamental variables in LDFT. The kinetic-, interaction-, and total-energy functionals $T = T[\eta_{k\sigma}]$, $W = W[\eta_{k\sigma}]$, and $E = E[\eta_{k\sigma}]$ depend solely on $\eta_{k\sigma}$. In particular, the kinetic-energy functional (6) is given by

$$T[\eta_{k\sigma}] = \sum_{\mathbf{k} \in \text{BZ}\sigma} \varepsilon_{\mathbf{k}} \eta_{k\sigma}, \quad (15)$$

where

$$\varepsilon_{\mathbf{k}} = \sum_{i=1}^{N_a} t(\mathbf{R}_i) \cos(\mathbf{k} \cdot \mathbf{R}_i) \quad (16)$$

is the tight-binding dispersion relation for $t_{ij} = t(\mathbf{R}_i - \mathbf{R}_j)$. The total energy

$$E[\eta_{k\sigma}] = \sum_{k\sigma} \varepsilon_{\mathbf{k}} \eta_{k\sigma} + W[\eta_{k\sigma}] \quad (17)$$

has to be minimized by keeping a fixed number of spin- σ electrons

$$N_\sigma = \sum_{\mathbf{k} \in \text{BZ}} \eta_{k\sigma}. \quad (18)$$

One therefore introduces the Lagrange functional

$$\mathcal{L}[\eta_{k\sigma}, \mu_\sigma] = E[\eta_{k\sigma}] - \sum_{\sigma} \mu_\sigma \left(\sum_{\mathbf{k} \in \text{BZ}} \eta_{k\sigma} - N_\sigma \right) \quad (19)$$

and solves the extremum condition $\partial \mathcal{L} / \partial \eta_{k\sigma} = 0$ for all $\mathbf{k}\sigma$.

III. RECIPROCAL-SPACE APPROXIMATION TO $W[\gamma]$ IN THE HUBBARD MODEL

In the following, we consider the single-band Hubbard model, which is given by

$$\hat{H} = \hat{T} + \hat{W} = \sum_{ij\sigma} t_{ij} \hat{c}_{i\sigma}^\dagger \hat{c}_{j\sigma} + U \sum_i \hat{n}_{i\uparrow} \hat{n}_{i\downarrow}. \quad (20)$$

In the usual notation, t_{ij} is the hopping integral between atoms or lattice sites located at \mathbf{R}_i and \mathbf{R}_j and U is the onsite Coulomb repulsion. The periodicity of the lattice and the s -like character of the local orbitals implies that $t_{ij} = t(|\mathbf{R}_i - \mathbf{R}_j|)$ depends only on the distance between the atoms i and j .

In order to derive a physically sound approximation to $W[\gamma]$ from a \mathbf{k} -space perspective, it is useful to consider two important limiting situations, for which Levy's constrained

minimization (7) can be exactly solved. The first one concerns idempotent density matrices, i.e., $\gamma_\sigma^2 = \gamma_\sigma$. It is easy to see that in this case the occupation numbers $\eta_{k\sigma}$ are 0 or 1, and that the only many-body state $|\psi\rangle$ which can yield this kind of γ is the Slater determinant made of the occupied natural orbitals $u_{ik\sigma}$. The corresponding interaction energy W is then equal to the Hartree-Fock energy

$$W_{\text{HF}} = \sum_{\substack{k k' \\ \text{occ}}} (W_{kk'kk'} - W_{kk'k'k}), \quad (21)$$

where $W_{kk'kk'}$ ($W_{kk'k'k}$) stands for the direct (exchange) Coulomb integrals between Bloch states. In particular for the Hubbard model we have $W_{\text{HF}} = U D_{\text{HF}}$, where

$$D_{\text{HF}} = \sum_{i k k'} \eta_{k\uparrow} \eta_{k'\downarrow} |u_{ik\uparrow}|^2 |u_{ik'\downarrow}|^2 = \sum_i \gamma_{ii\uparrow} \gamma_{ii\downarrow} \quad (22)$$

is the uncorrelated average number of double occupations for the spin-density distribution $\gamma_{ii\sigma}$. Since the many-body eigenstates of the kinetic-energy operator \hat{T} are simple Slater determinants, the ground state γ is idempotent in the limit of vanishing interactions, provided that degeneracies are absent. However, if there are degeneracies not arising from spin (i.e., at the Fermi energy of the single-particle spectrum $\varepsilon_{\mathbf{k}}$) one usually finds fractional occupation numbers and a reduced $W < W_{\text{HF}}$, even for arbitrary weak interactions.

The other important limit is given by the scalar density matrices $\gamma_\sigma = n_\sigma \mathbb{1}$, where $n_\sigma = N_\sigma/N_a$ is the density of spin- σ electrons. In this case, the occupation numbers $\eta_{k\sigma} = n_\sigma$ are independent of \mathbf{k} . In order to represent a scalar γ one may construct symmetrized localized states where charge fluctuations are suppressed and the interaction energy is minimal. For the Hubbard model one thus obtains $W_\infty = U D_\infty$, where

$$D_\infty = \begin{cases} 0 & \text{if } N_e \leq N_a, \\ N_e - N_a & \text{if } N_e > N_a \end{cases} \quad (23)$$

is the minimal number of double occupations. Scalar density matrices are most relevant in the limit of strong interactions or vanishing hopping integrals, particularly at half-band filling where the ground-state kinetic energy tends to zero.

Notice that the above considerations are independent of the actual form of the natural orbitals $u_{ik\sigma}$. The discussed limits allow us to quantify the changes in W as a function of $\eta_{k\sigma}$, from integer occupations $\eta_{k\sigma} = 0$ or 1 to \mathbf{k} -independent occupations $\eta_{k\sigma} = n_\sigma$. They also provide information on the dependence of W on $u_{ik\sigma}$ in the limits of weak and strong correlations. Nevertheless, describing the behavior of W for intermediate γ remains a challenge.

In order to interpret and approximate W for arbitrary $\eta_{k\sigma}$, it is useful to consider the independent-fermion entropy (IFE)

$$S[\eta_{k\sigma}] = - \sum_{k\sigma} [\eta_{k\sigma} \ln(\eta_{k\sigma}) + (1 - \eta_{k\sigma}) \ln(1 - \eta_{k\sigma})], \quad (24)$$

which corresponds to an arbitrary occupation-number distribution $\eta_{k\sigma}$ of the natural orbitals, i.e., not necessarily the equilibrium one [71]. On the one side, if the electrons are uncorrelated, we have $\eta_{k\sigma} = 0$ or 1 and therefore $S = 0$. This is the minimum possible value of S regarded as a functional of

$\eta_{k\sigma}$. On the other side, if the electrons are localized, we have $\eta_{k\sigma} = n_\sigma = N_\sigma/N_a$ for all \mathbf{k} , which implies that S takes its maximum possible value S_∞ for the given number of spin- σ electrons N_σ . At half-band filling we have $(n_\uparrow + n_\downarrow) = 1$ and S_∞ can be written as

$$S_\infty = -2N_a[n_\uparrow \ln(n_\uparrow) + n_\downarrow \ln(n_\downarrow)]. \quad (25)$$

It is interesting to notice that the distributions of $\eta_{k\sigma}$ which yield the extreme values of the interaction energy W for fixed $u_{ik\sigma}$ also correspond to the extreme values of the IFE. This suggests that $S[\eta_{k\sigma}]$ could be used as a measure of the degree of electron correlations, by means of which the functional dependence of $W[\eta_{k\sigma}]$ could be efficiently approximated.

In order to quantify the relation between $W[\gamma]$ and $S[\gamma]$, we have determined W exactly for the half-filled Hubbard model by performing Levy's minimization (7) for periodic $\gamma_{ij\sigma}$ [see Eqs. (13) and (14)]. This requires introducing Lagrange multipliers λ_{ij} in order to ensure that $|\psi\rangle$ gives the desired fixed values of $\gamma_{ij\sigma}$. As shown in Ref. [59], the λ_{ij} take the role of interatomic hoppings in the Euler-Lagrange eigenvalue equations giving the minimum $\langle\psi|\hat{W}|\psi\rangle$. In practice, one assumes different ratios between the λ_{ij} at different distances, which correspond to one-dimensional (1D) and two-dimensional (2D) lattices having first and second NN λ_{ij} . The overall values of λ_{ij} are then scaled from $\lambda_{ij} = 0$ to $\lambda_{ij} \gg U$ in order to obtain different occupation-number distributions $\eta_{k\sigma}$ and thereby scan the complete range of values of S , from weak to strong correlations ($0 \leq S \leq S_\infty$). For not too large finite systems, the ground-state Hubbard problem resulting from the minimization in Eq. (7) can then be solved by using the Lanczos method [72,73]. Once the many-body state $|\psi\rangle$ yielding the minimum $\langle\psi|\hat{W}|\psi\rangle$ has been found, it is straightforward to calculate the corresponding $\gamma_{ij\sigma}$ from Eq. (4). The natural orbital occupations $\eta_{k\sigma}$ are obtained by diagonalizing $\gamma_{ij\sigma}$ or by direct Fourier transformation [see Eq. (14)]. In this way, the functional relation between W and $\gamma_{ij\sigma}$, or between W and $\eta_{k\sigma}$, is established. For each occupation-number distribution $\eta_{k\sigma}$, the corresponding $S[\eta_{k\sigma}]$ follows directly from Eq. (24).

Figure 1 shows the relation between the interaction energy $W[\eta_{k\sigma}]$ and the independent-fermion entropy $S[\eta_{k\sigma}]$ for a number of 1D and 2D half-filled lattices having different numbers of atoms $N_a \leq 12$ and different occupation-number distributions $\eta_{k\sigma}$. Remarkably, the simple $S[\eta_{k\sigma}]$ captures most of the dependence of W on $\eta_{k\sigma}$. One observes indeed that the relation between W and S is approximately independent of the size and dimension of the system, and of the precise form of the distribution $\eta_{k\sigma}$. The deviations from the common approximately linear trend are always small (below 10%). Therefore, we propose to approximate $W[\eta_{k\sigma}]$ by a simple function

$$W = W(S[\eta_{k\sigma}]) \quad (26)$$

of the IFE given by Eq. (24). The relation between W and S appears to be close to linear over a wide range of values of S , at least for the considered half-filled cases. Nevertheless, some deviations from the linear behavior are found for very small S , where the orbital occupations are close to integer (see Fig. 1). For simplicity, we shall use a linear approximation to $W(S)$ in the applications discussed in Sec. IV.

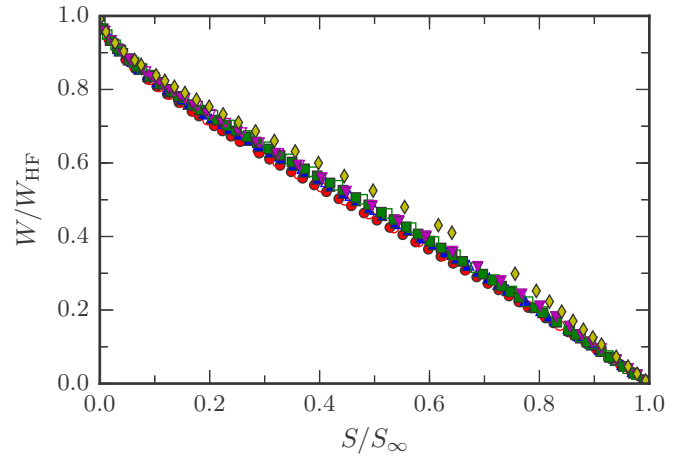


FIG. 1. Relation between the exact interaction energy $W[\eta_{k\sigma}]$ of the periodic half-filled Hubbard model and the independent Fermion entropy $S[\eta_{k\sigma}]$ corresponding to different natural-orbital occupation distributions $\eta_{k\sigma}$. The results are obtained from Lanczos diagonalizations on finite 1D rings having $N_a = 6$ (circles), $N_a = 10$ (upright triangles) and $N_a = 14$ (squares), as well as for finite 2D square-lattice rectangles having $N_a = 2 \times 4$ (downright triangles) and $N_a = 3 \times 4$ (diamonds) with periodic boundary conditions. The solid symbols correspond to first NN hoppings t_{01} , while the open symbols also include second NN hoppings $t_{02} = t_{01}/2$.

It is important to keep in mind that assuming that W depends on $\eta_{k\sigma}$ only through S remains an approximation, irrespectively of the detail by which $W(S)$ may be interpolated. In fact, Eq. (26) imposes some restrictions on the \mathbf{k} dependence of the ground state $\eta_{k\sigma}$, which deserve to be clarified. Let us assume that the interaction energy is some arbitrary function $W = W(S)$ of the IFE. Replacing W in Eq. (17), the Euler-Lagrange equations $\partial\mathcal{L}/\partial\eta_{k\sigma} = 0$ yield the ground-state occupation numbers

$$\eta_{k\sigma} = \frac{1}{1 + e^{(\varepsilon_k - \mu_\sigma)/\vartheta}}, \quad (27)$$

where

$$\vartheta = -\frac{dW}{dS} \quad (28)$$

plays the role of an effective temperature, which is common to all $\mathbf{k}\sigma$. Notice that ϑ changes with the form of $W(S)$ and with the actual ground-state value of S . The spin-dependent chemical potential μ_σ is chosen to reproduce the total number of spin- σ electrons according to Eq. (18). Clearly, the set of equations (27) has to be solved self-consistently for all $\mathbf{k}\sigma$ together with Eqs. (18) and (28) since ϑ depends on the distribution $\eta_{k\sigma}$ through S , and μ_σ depends on ϑ . Thus, the relation between $\eta_{k\sigma}$ and the single-particle band structure ε_k varies as a function of the Coulomb interaction U through the effective temperature ϑ . Let us recall that W scales linearly with U and therefore $\vartheta = -U dD/dS$, where D is the average number of double occupations. Aside from the quantitative aspects, to be discussed in detail in Sec. IV, we may already conclude that the assumption $W = W(S)$ always implies that $\eta_{k\sigma}$ follows the Fermi-Dirac distribution since neither ϑ nor μ_σ depend on $\mathbf{k}\sigma$. This means that $\eta_{k\sigma}$ is a continuous function

of ε_k , except in the uncorrelated case ($U = 0$). Fermi-liquid behavior, with a discontinuity in $\eta_{k\sigma}$ at μ_σ , or Luttinger-liquid behavior, showing a diverging derivative of $\eta_{k\sigma}$ at μ_σ , cannot be described by this approximation. And still, despite these restrictions, we shall be able to show that already the most simple entropy-based ansatz for $W[\eta_{k\sigma}]$ gives a quite accurate account of the ground-state properties of the half-filled Hubbard model, particularly in the strongly correlated limit.

For the following applications, we propose to approximate $W[\eta_{k\sigma}]$ by the simple linear relation

$$W[\eta_{k\sigma}] = W_{\text{HF}} \left(1 - \frac{S[\eta_{k\sigma}]}{S_\infty} \right), \quad (29)$$

where

$$W_{\text{HF}} = U D_{\text{HF}} = U \sum_i \gamma_{i\uparrow} \gamma_{i\downarrow} \quad (30)$$

is the Hartree-Fock Coulomb energy and S_∞ is the upper bound for $S[\eta_{k\sigma}]$ given by Eq. (25). Substituting Eq. (29) into Eq. (17), and using that in the homogeneous case $W_{\text{HF}} = U N_a n_\uparrow n_\downarrow$, one obtains the energy functional

$$E[\eta_{k\sigma}] = \sum_{k\sigma} \varepsilon_k \eta_{k\sigma} + U N_a n_\uparrow n_\downarrow \left(1 - \frac{S[\eta_{k\sigma}]}{S_\infty} \right) \quad (31)$$

$$= \sum_{k\sigma} \varepsilon_k \eta_{k\sigma} + W_{\text{HF}} - \vartheta S[\eta_{k\sigma}], \quad (32)$$

with the effective temperature $\vartheta = -dW/dS = U N_a n_\uparrow n_\downarrow / S_\infty$. A simple physical interpretation follows. In the present linear ansatz, the correlation energy $W - W_{\text{HF}}$ of the interacting problem having occupation numbers $\eta_{k\sigma}$ is approximated by the entropy contribution $-\vartheta S$ to the Helmholtz free energy of an auxiliary noninteracting system at an effective finite temperature ϑ , which is proportional to U . In this way, fractional occupations $\eta_{k\sigma}$ are obtained in the ground state of all interacting systems ($U \neq 0$).

IV. RESULTS AND DISCUSSION

In this section we apply the linear IFE approximation of the interaction-energy functional to the half-filled Hubbard model on one-, two-, and three-dimensional lattices. First, we consider finite systems with periodic boundary conditions and compare the calculated ground-state properties with the outcome of exact Lanczos diagonalizations. Second, we investigate the one-dimensional infinite chain for which the exact Bethe-ansatz solution is available. Third, we apply the method to the Hubbard model on the 2D square lattice, the 3D cubic lattice, and the limit of infinite dimensions. Finally, spin-polarized systems are considered.

A. Finite periodic rings

In Fig. 2, results are given for several ground-state properties of a ring with $N_a = 14$ sites and $N_\uparrow = N_\downarrow = 7$ electrons as a function of the Coulomb interaction strength U/t . These were obtained either by using the IFE approximation to LDFT or by exact numerical Lanczos diagonalizations. Figure 2(a) shows that the proposed ansatz for W reproduces the ground-state energy E_0 very accurately for all U/t . The discrepancies between

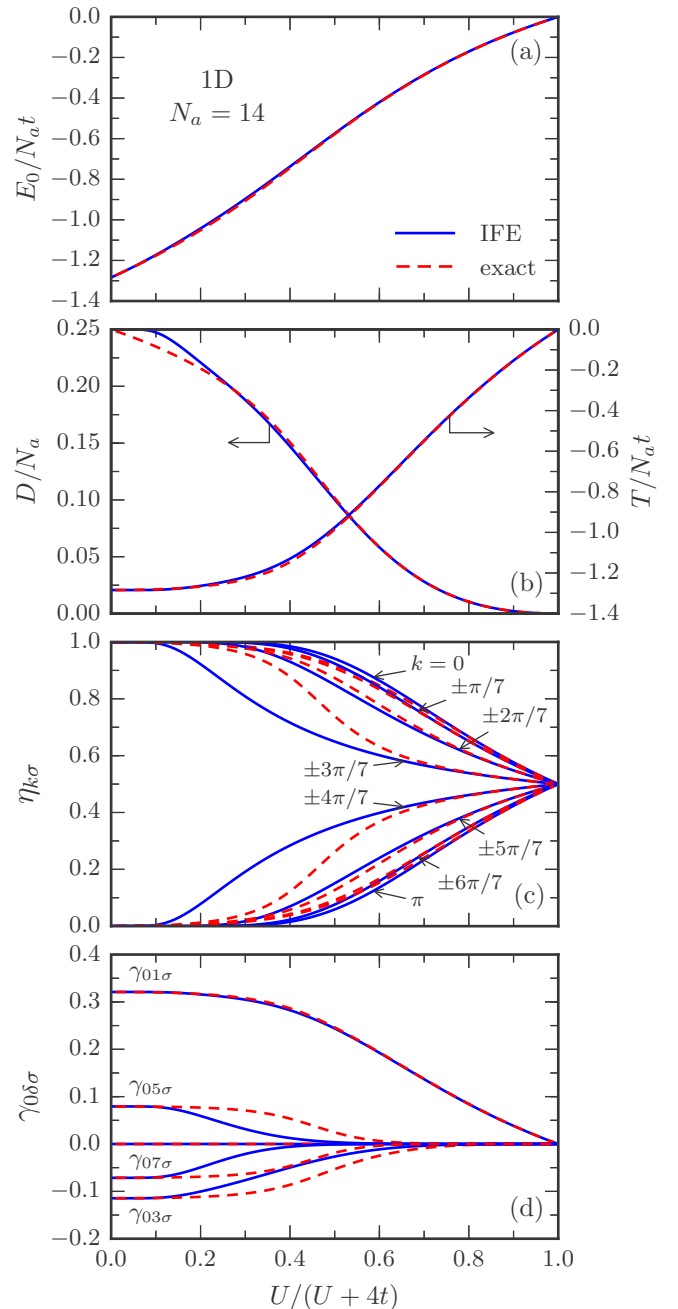


FIG. 2. Ground-state properties of the 1D Hubbard model on a ring having $N_a = 14$ sites and $N_\uparrow = N_\downarrow = 7$ electrons as a function of the Coulomb-repulsion strength U/t . The linear independent-fermion entropy (IFE) ansatz (blue full curves) is compared with exact numerical Lanczos diagonalizations (red dashed curves): (a) ground-state energy E_0 , (b) average number of double occupations D and kinetic energy T , (c) natural-orbital occupation numbers $\eta_{k\uparrow} = \eta_{k\downarrow}$, and (d) density-matrix elements $\gamma_{0\delta\uparrow} = \gamma_{0\delta\downarrow}$ between an atom $i = 0$ and its δ th-nearest neighbor.

IFE and exact results are always less than 1.2%. In particular in the strongly correlated limit we obtain $E_0/N_a = -\alpha t^2/U$ with $\alpha_{\text{IFE}} = 2.77$, while the exact result is $\alpha_{\text{ex}} = 2.79$. This demonstrates the ability of LDFT and the IFE ansatz to account for the Heisenberg limit of the Hubbard model, where the energies associated to spin and charge degrees of freedom

are widely separated. Moreover, it is important to remark that the accuracy in E_0 is not the consequence of a significant compensation of errors. Indeed, as shown in Fig. 2(b), very good results are obtained for both the average number of double occupations D and the kinetic energy T . Only in the weakly correlated limit ($U/t < 1$) we find that the IFE calculations overestimate D by remaining too close to $D_{\text{HF}} = N_a/4$. This reflects inaccuracies in our approximation to $W[\eta_{k\sigma}]$ for nearly integer $\eta_{k\sigma}$, which can be partly ascribed to the deviations from linearity in $W(S)$ for small S , as already observed in the context of Fig. 1. The results for D for small U/t can in fact be improved by adapting the dependence of W as a function of S for small S . However, a systematic universal way of developing such improvements is not known at present. It is also possible that these inaccuracies are intrinsic to the IFE ansatz (26). In any case, the small errors in D do not affect E_0 significantly since for small U/t the kinetic contribution T dominates, for which very accurate results are obtained.

In addition to the average kinetic and Coulomb energies, it is important to evaluate the ground-state density matrix γ^0 which minimizes the energy functional $E[\gamma]$. A first insight from a k -space perspective is provided by Fig. 2(c), where the ground-state occupation numbers $\eta_{k\sigma}$ are shown as functions of the interaction strength U/t . In the 14-atom ring, there are eight distinct curves for $\eta_{k\sigma}$, which correspond to $k = 0$, $k = \pm v\pi/7a$ with $v = 1-6$ and $k = \pi/a$, as implied by time inversion symmetry (i.e., $\eta_{k\sigma} = \eta_{-k\sigma} \forall k$). Taking into account Eq. (27) and the fact that the k dependence of the single-particle spectrum ε_k respects the point-group symmetry of the lattice, one concludes that the $\eta_{k\sigma}$ derived from any IFE approximation of the form (26) always satisfies the local symmetry properties of the model.

Another fundamental property of the average Bloch-state occupations may be inferred from the electron-hole symmetry of the half-filled Hubbard model on bipartite lattices. In this case, one can show that

$$\eta_{k\sigma} = 1 - \eta_{k+q,\sigma}, \quad (33)$$

where q satisfies $\varepsilon_{k+q} = -\varepsilon_k$. In the 1D chain we have $q = \pi$ and in general one finds $q = \sum_{i=1}^d \mathbf{b}_i/2$, where \mathbf{b}_i denotes the different elementary vectors of the reciprocal lattice [see Eq. (16)]. To prove the relation (33), one can first show that the Hubbard Hamiltonian \hat{H} is invariant under the electron-hole transformation $\hat{h}_{k\sigma}^\dagger = \hat{c}_{k+q,\sigma}$. The eigenstates of \hat{H} can then be chosen to be eigenstates of the electron-hole transformation whose eigenvalues are ± 1 . In particular, for the ground state $|\psi_0\rangle$ we have

$$\begin{aligned} \langle \psi_0 | \hat{c}_{k\sigma}^\dagger \hat{c}_{k\sigma} | \psi_0 \rangle &= \langle \psi_0 | \hat{h}_{k\sigma}^\dagger \hat{h}_{k\sigma} | \psi_0 \rangle \\ &= \langle \psi_0 | 1 - \hat{c}_{k+q,\sigma}^\dagger \hat{c}_{k+q,\sigma} | \psi_0 \rangle, \end{aligned} \quad (34)$$

which coincides with Eq. (33). From the perspective of LDFT it is interesting to observe that the IFE approximation (26) always satisfies the electron-hole symmetry since $\varepsilon_{k+q} = -\varepsilon_k$, combined with Eq. (27), implies Eq. (33).

Quantitatively, one observes that in most cases the IFE approximation reproduces quite accurately the U/t dependence of the occupation numbers. For $U/t \ll 1$ one obtains, as expected, $\eta_{k\sigma} = 1$ for $|k| \leq \pi/2$ and $\eta_{k\sigma} = 0$ otherwise. As the Coulomb repulsion increases, charge fluctuations

are progressively suppressed in order to reduce double occupations. Thus, $\eta_{k\sigma}$ decreases (increases) for $|k| < \pi/2$ ($|k| > \pi/2$) until $\eta_{k\sigma} \rightarrow 1/2$ for all $k\sigma$ in the strongly correlated limit ($U/t \rightarrow \infty$). Notice, however, that our ansatz underestimates (overestimates) $\eta_{k\sigma}$ for $|k| = 3\pi/7$ ($|k| = 4\pi/7$) and intermediate interaction strength. These values of k correspond to the smallest $|\varepsilon_k|$. In other words, the approximation overestimates the excitation of electrons across the Fermi energy $\varepsilon_F = 0$. This could be a consequence of the relatively small slope of the Fermi distribution in the vicinity of ε_F . In fact, in the thermodynamic limit, the derivative of $\eta_{k\sigma}$ is expected to diverge for $\varepsilon_k = \varepsilon_F$, as in a Luttinger liquid [74].

The occupation numbers $\eta_{k\sigma}$ are related to the density-matrix elements $\gamma_{ij\sigma}$ by a standard Fourier transformation. Since $\gamma_{ij\sigma}$ depends only on the interatomic distance, it is sufficient to consider only the matrix elements of the form $\gamma_{0\delta\sigma}$ between an atom $i = 0$ and its δ th-nearest neighbor. Notice that in half-filled bipartite lattices $\gamma_{0\delta\sigma}$ vanishes between sites belonging to the same sublattice. In the 1D chain, this means $\gamma_{0\delta\sigma} = 0$ for even δ . The statement can be shown using Eq. (33) by expressing $\gamma_{ij\sigma}$ as the Fourier transform of $\eta_{k\sigma}$. Alternatively, one may consider the electron-hole transformation $\hat{h}_{i\sigma}^\dagger = \pm \hat{c}_{i\sigma}$, where the positive sign applies to the sites on one of the sublattices and the negative sign to the other sublattice. Since the Hubbard model is invariant upon this transformation, the eigenstates of \hat{H} can be chosen to respect this symmetry, i.e., to remain unchanged or simply change sign upon replacing all electrons by holes. Thus, we have $\langle \psi_0 | \hat{c}_{i\sigma}^\dagger \hat{c}_{j\sigma} | \psi_0 \rangle = \langle \psi_0 | \hat{h}_{i\sigma}^\dagger \hat{h}_{j\sigma} | \psi_0 \rangle$ for all $i \neq j$. In particular, when i and j belong to the same sublattice we have $\hat{c}_{i\sigma}^\dagger \hat{c}_{j\sigma} = \hat{h}_{i\sigma}^\dagger \hat{h}_{j\sigma} = -\hat{h}_{j\sigma}^\dagger \hat{h}_{i\sigma}$, which implies $\gamma_{ij\sigma} = -\gamma_{ji\sigma} = 0$ since $\gamma_{ij\sigma}$ is real. A similar argument shows that any IFE approximation of the form (26) also fulfills this symmetry. In fact, since \hat{H} is invariant under the given electron-hole transformation, the single-particle energies $\varepsilon_k^{(h)}$ of the holes coincide with the corresponding single-particle energies ε_k of the electrons. Moreover, since the number of electrons N_σ and the number of holes $N_\sigma^{(h)}$ are the same for $N_\uparrow = N_\downarrow = N_a/2$, the chemical potential for electrons and holes are also the same (i.e., $\mu_\sigma^{(h)} = \mu_\sigma$). Equation (27) implies that in the IFE approximation $\eta_{k\sigma}^{(h)} = \eta_{k\sigma}$ and accordingly $\gamma_{ij\sigma}^{(h)} = \gamma_{ij\sigma}$ [see Eq. (14)]. Finally, it follows that $\gamma_{ij\sigma} = 0$ when i and j belong to the same sublattice.

The four distinct nonvanishing elements $\gamma_{0\delta\sigma}$ having δ odd in the 14-atom ring are shown in Fig. 2(d). The IFE results are in good qualitative agreement with the exact ones. However, for intermediate values of U/t our approximation underestimates the delocalization of the electrons beyond first NNs (i.e., $\gamma_{03\sigma}$, $\gamma_{05\sigma}$, and $\gamma_{07\sigma}$). For example, for $U/t = 4$, the calculated $|\gamma_{03\sigma}|$ is about 50% smaller than the exact result, while $\gamma_{05\sigma}$ and $\gamma_{07\sigma}$ nearly vanish. Although the correlation-induced localization is qualitatively explained, the localization length is underestimated. The discrepancies in $\gamma_{0\delta\sigma}$ ($\delta \geq 3$) seem more severe from a local perspective than what one might have expected on the basis of the Fourier transform $\eta_{k\sigma}$. As shown in Fig. 2(c), the IFE approximation to $\eta_{k\sigma}$ is quite accurate except for $k = \pm 3\pi/7$ and $\pm 4\pi/7$. Let us finally observe that the IFE results for the NN $\gamma_{01\sigma}$ are very good for all U/t . Also, the variance $\Delta k = \sqrt{\langle k^2 \rangle}$, which increases

monotonously with U/t as a result of localization, is precisely reproduced. This is consistent with the very good accuracy of the calculated kinetic energy, which is proportional to $\gamma_{01\sigma}$.

B. Finite systems in two dimensions

In Fig. 3, results are given for the ground-state properties of the half-filled Hubbard model on a 4×4 2D square-lattice cluster with periodic boundary conditions ($N_\uparrow = N_\downarrow = 8$). Comparison with exact Lanczos diagonalizations shows that the performance of the linear IFE approximation in two dimensions is similar to the 1D case. The ground-state energy E_0 is accurately reproduced for all values of U/t . In the strongly correlated limit, we find $E_0/N_a \simeq -\alpha t^2/U$ which correctly reproduces the behavior of localized Heisenberg spins [74,75]. The obtained $\alpha_{\text{IFE}} = 5.55$ is only 13% larger than the exact result $\alpha_{\text{ex}} = 4.81$ deduced from the Lanczos diagonalizations. The binding energy $|E_0|$ is somewhat overestimated for intermediate values of U/t . This is mainly due to the overestimation of the kinetic-energy gain $|T|$, which turns out to be slightly less accurate than in 1D [compare Figs. 2(b) and 3(b)]. The average number of double occupations is very close to the exact result, except for $U/t < 2$, where it is underestimated up to 30% for $U/t = 0$. Although the impact of D on E_0 is not very important for small U/t , the linear increase of E_0 for small values of U is underestimated.

Notice that both the exact and IFE values for D are smaller than $D_{\text{HF}} = N_a/4$ for $U = 0$. This is a consequence of the degeneracy of the single-particle spectrum of the periodic 4×4 cluster at the Fermi energy $\varepsilon_F = 0$. It implies that some of the average natural-orbital occupations are fractional even for $U = 0$, namely, for those \mathbf{k} having $\varepsilon_{\mathbf{k}} = \varepsilon_F = 0$. There are in fact six Bloch states at ε_F [$\mathbf{k} = (\pm\pi/2, \pm\pi/2)$, $(\pi, 0)$, and $(0, \pi)$]. These are occupied by 6 electrons when $U = 0$, the remaining 10 electrons occupy the $\mathbf{k} = 0$, $\mathbf{k} = (\pm\pi/2, 0)$, and $\mathbf{k} = (0, \pm\pi/2)$ orbitals. As shown in Fig. 3(c), both exact and IFE calculations yield $\eta_{k\sigma} = 1/2$ for \mathbf{k} lying on the Fermi surface, irrespectively of the value of U/t . This corresponds to an equal occupation of all states having the same $\varepsilon_{\mathbf{k}}$ and is consistent with the idea behind our ansatz, that increasing the IFE associated to the natural orbital occupations should reduce the Coulomb-repulsion energy. Nevertheless, the linear IFE ansatz happens to be too simple to yield a very accurate D for small U/t , even if the $\eta_{k\sigma}$'s are almost exactly obtained.

As in the 1D case, the average occupation of the single-particle levels below (above) ε_F decreases (increases) as U/t increases, starting from $\eta_{k\sigma} = 1$ ($\eta_{k\sigma} = 0$) at $U/t = 0$. Figure 3(c) shows that the $\eta_{k\sigma}$ calculated with the linear IFE ansatz are remarkably accurate for all $\mathbf{k}\sigma$ and in the whole range of U/t . The approximation respects in particular the invariance of $\eta_{k\sigma}$ with respect to the rotations and reflections of \mathbf{k} that describe the lattice point-group symmetry since the dispersion relation $\varepsilon_{\mathbf{k}}$ fulfills these symmetries. In the square lattice the electron-hole symmetry takes the form $\eta_{k\sigma} = \eta_{k\pm(\pi,\pi),\sigma}$. This implies that $\gamma_{ij\sigma} = 0$ when i and j belong to the same sublattice, in agreement with the exact solution.

Results for $\gamma_{ij\sigma}$ are shown in Fig. 3(d) as a function of U/t . The point-group symmetry of the square lattice requires that, for given values $m, n \in \mathbb{Z}$, the density-matrix elements between the lattice site at $(0,0)$ and any of the lattice sites at

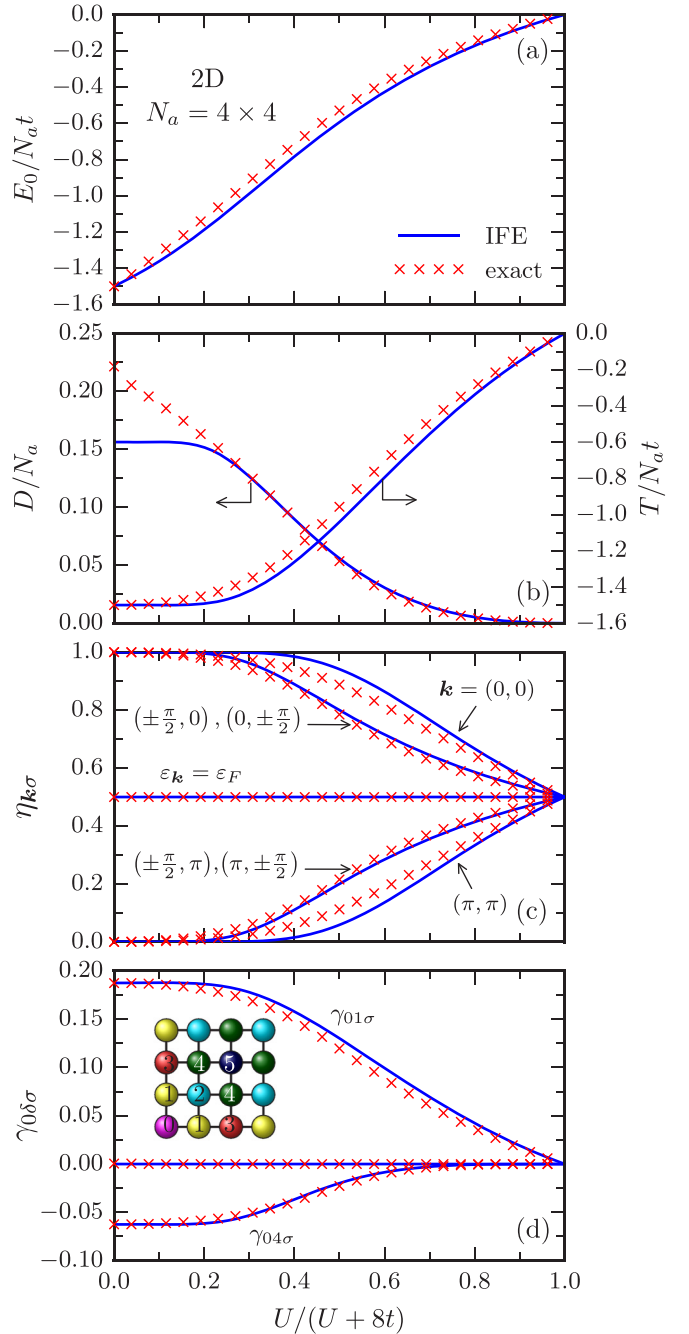


FIG. 3. Ground-state properties of the 2D Hubbard model on a 4×4 square lattice with $N_\uparrow = N_\downarrow = 8$ electrons and periodic boundary conditions. Results are given for the linear independent-fermion entropy (IFE) ansatz (blue full curves) and exact Lanczos diagonalizations (crosses) as a function of the Coulomb-repulsion strength U/t : (a) ground-state energy E_0 , (b) average number of double occupations D and kinetic energy T , (c) natural-orbital occupation numbers $\eta_{k\uparrow} = \eta_{k\downarrow}$, and (d) density-matrix elements $\gamma_{0\delta\uparrow} = \gamma_{0\delta\downarrow}$ between an atom $i = 0$ and its δ th-nearest neighbor, as illustrated in the inset.

$(\pm m, \pm n)$ or $(\pm n, \pm m)$ (in units of the lattice parameter a) are all the same (single-band s -like model). Therefore, only the curves for $\gamma_{0\delta\sigma}$ between an atom 0 and its δ th-nearest neighbor are shown. Notice that all the $\gamma_{0\delta\sigma}$ obtained with the IFE

approximation closely follow the exact numerical calculations for all U/t . In particular, the correlation-induced localization is very well reproduced. The results are in fact significantly more accurate than in 1D, at least for the short range which can be explored within a finite cluster [see also Fig. 2(d)].

In order to explore magnetically frustrated systems in the framework of LDFT, we consider a 4×4 cluster of the triangular 2D lattice with periodic boundary conditions. In Fig. 4, the IFE results for several ground-state properties are compared with the corresponding exact Lanczos diagonalizations. One observes that the ground-state energy E_0 is fairly well reproduced as a function of U/t . However, the binding is systematically overestimated, particularly for intermediate interaction strengths (e.g., $E_0^{\text{ex}} - E_0^{\text{IFE}} = 0.21N_a t$ for $U/t = 9.33$). In the strongly correlated limit, the IFE approximation yields the correct linear dependence on Heisenberg's coupling J between localized spins: $E_0/N_a \simeq -\alpha t^2/U$. However, the obtained proportionality constant $\alpha_{\text{IFE}} = 8.32$ is significantly larger than the exact one ($\alpha_{\text{ex}} = 5.14$).

The average number of double occupations D obtained with the IFE approximation is fairly close to the exact calculation, except for $U/t \lesssim 4$ where it is underestimated by up to 27% for $U/t = 0$. This is a consequence of the large (ninefold) degeneracy of the Fermi level of the 4×4 cluster, which is filled with only two electrons. Under these circumstances, the IFE approximation overestimates the ability of the finite many-body system to take advantage of the degeneracy at ε_F and suppress part of the double occupations. Nevertheless, the underestimation of D has little impact on the Coulomb and total ground-state energies since U/t is relatively small. A similar behavior has been observed for the square lattice.

The natural orbitals or Bloch states $u_{i\mathbf{k}\sigma}$ having different wave vectors \mathbf{k} may be classified in two groups: those having the lowest single-particle energies $\varepsilon_{\mathbf{k}}$, which are fully occupied in the uncorrelated limit ($\eta_{\mathbf{k}\sigma} = 1$), and those which have larger $\varepsilon_{\mathbf{k}}$ and are weakly occupied for $U = 0$ (in average $\bar{\eta}_{\mathbf{k}\sigma} = \frac{1}{9}$). The latter fractional occupations for $U \rightarrow 0$ are a consequence of the degeneracy of the single-particle spectrum of the 4×4 triangular cluster, which at half-band filling holds two electrons with opposite spins in the ninefold-degenerate Fermi level. Notice that the exact natural orbital occupations deviate from the average $\bar{\eta}_{\mathbf{k}\sigma} = \frac{1}{9}$ [Fig. 4(c)]. This is a subtle finite-size effect of the electronic correlations, which manage to completely suppress the Hubbard interaction between the two electrons at ε_F even for arbitrarily small U/t . As in the previously considered bipartite lattice, the occupations of the Bloch states having $\eta_{\mathbf{k}\sigma} = 1$ for $U = 0$ decrease monotonously with increasing U/t , whereas the occupations of the other Bloch states, having small $\eta_{\mathbf{k}\sigma}$, increase monotonously [see Fig. 4(c)]. Finally, in the localized limit ($U/t \rightarrow \infty$) one obtains, as expected, $\eta_{\mathbf{k}\sigma} = \frac{1}{2}$ for all \mathbf{k} . The IFE approximation correctly reproduces the trends in $\eta_{\mathbf{k}\sigma}$ as a function U/t . However, it somewhat overestimates (underestimates) $\eta_{\mathbf{k}\sigma}$ for the orbitals having $\eta_{\mathbf{k}\sigma} \geq \frac{1}{2}$ ($\eta_{\mathbf{k}\sigma} \leq \frac{1}{2}$) as the interaction strength increases ($U/t > 8$). Notice, moreover, that in any IFE ansatz for W the ground state $\eta_{\mathbf{k}\sigma}$'s are always the same for all the Bloch states having the same single-particle energy $\varepsilon_{\mathbf{k}}$. Consequently, our approximation cannot resolve the above-discussed differences in $\eta_{\mathbf{k}\sigma}$ among degenerate natural orbitals. Nevertheless, the IFE results compare very

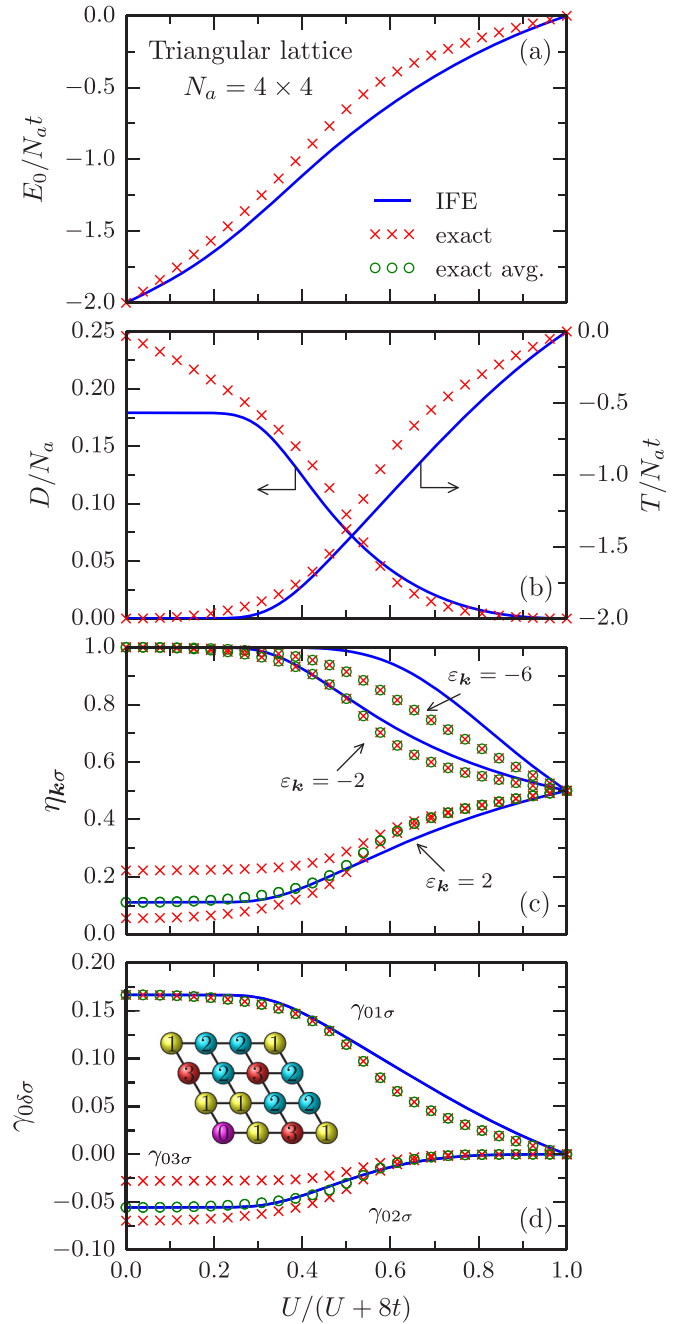


FIG. 4. Ground-state properties of the half-filled 2D Hubbard model on a 4×4 triangular lattice with periodic boundary conditions as functions of the Coulomb-repulsion strength U/t . Results are given for the linear independent-fermion entropy (IFE) ansatz (blue full curves) and exact Lanczos diagonalization (crosses): (a) ground-state energy E_0 , (b) average number of double occupations D and kinetic energy T , (c) natural-orbital occupation numbers $\eta_{\mathbf{k}\sigma} = \eta_{\mathbf{k}\downarrow}$, and (d) density-matrix elements $\gamma_{0\delta\uparrow} = \gamma_{0\delta\downarrow}$ between an atom 0 and its δ th-nearest neighbor (see inset). The open circles in (c) and (d) show the average of the exact results over the \mathbf{k} vectors having the same single-particle energy $\varepsilon_{\mathbf{k}}$.

well with the green open circles, which represent the exact average of $\eta_{\mathbf{k}\sigma}$ among the Bloch states having the same $\varepsilon_{\mathbf{k}}$. Taking into account that the accidental degeneracies become irrelevant as the system size grows, one expects that the IFE

approximation should yield more accurate occupations $\eta_{k\sigma}$ in the thermodynamic limit.

In Fig. 4(d) the density-matrix elements $\gamma_{0\delta}$ between an atom 0 and its δ th-nearest neighbor is reported as a function of U/t . One observes that the IFE approximation is in good qualitative agreement with the exact numerical calculations. The most significant discrepancies appear for small U/t , where the differences in $\gamma_{0\delta}$ between some atoms that are further apart ($\delta = 2$ and 3) cannot be resolved. This is a consequence of the above-discussed finite-size correlation effects and the resulting specific dependence of $\eta_{k\sigma}$ on \mathbf{k} . In sum, comparison between Figs. 3 and 4 shows that the overall accuracy of the IFE approximation in magnetically frustrated systems (e.g., the triangular 2D lattice) is similar, though in general somewhat less good than in bipartite lattices such as the square lattice.

C. Infinite periodic lattices

The purpose of this section is to investigate the properties of the half-filled Hubbard model on infinite periodic lattices by using the linear IFE approximation to LDFT. To be explicit, we focus on hypercubic lattices with NN hopping $-t_d < 0$, whose single-particle dispersion relation is given by

$$\varepsilon_{\mathbf{k}} = -\frac{2t}{\sqrt{d}} \sum_{\alpha=1}^d \cos(k_{\alpha}), \quad (35)$$

where $k_{\alpha} \in (-\pi, \pi]$ are the components of the wave vector \mathbf{k} in the d -dimensional BZ, measured in units of the inverse lattice parameter $1/a$. Notice that we have scaled the NN hopping integrals as $t_d = t/\sqrt{d}$ in order to ensure that the second moment

$$w_2 = \int \varepsilon^2 \rho(\varepsilon) d\varepsilon = 2d t_d^2 = 2t^2 \quad (36)$$

of the single-particle local density of states (DOS) per spin

$$\rho(\varepsilon) = \frac{1}{(2\pi)^d} \int_{\text{BZ}} \delta(\varepsilon - \varepsilon_{\mathbf{k}}) d^d k \quad (37)$$

is independent of d . This allows us to compare the results for different dimensions on the same footing and thus explore the limit of infinite dimensions.

The Bloch-state occupation numbers in the IFE approximation are given by the Fermi distribution

$$\eta_{k\sigma} = \eta_{\sigma}(\varepsilon_{\mathbf{k}}) = \frac{1}{1 + e^{(\varepsilon_{\mathbf{k}} - \mu_{\sigma})/\vartheta}}, \quad (38)$$

where the effective temperature

$$\vartheta = \frac{W_{\text{HF}}}{S_{\infty}} = -\frac{U n_{\uparrow} n_{\downarrow}}{2[n_{\uparrow} \ln(n_{\uparrow}) + n_{\downarrow} \ln(n_{\downarrow})]} \quad (39)$$

is independent of S in the linear approximation [see Eqs. (28) and (29)]. The chemical potential μ_{σ} is defined by the usual constraint

$$n_{\sigma} = \int \eta_{\sigma}(\varepsilon) \rho(\varepsilon) d\varepsilon. \quad (40)$$

The kinetic energy is given by

$$\frac{T}{N_a} = \sum_{\sigma} \int \varepsilon \eta_{\sigma}(\varepsilon) \rho(\varepsilon) d\varepsilon \quad (41)$$

and the independent-fermion entropy by

$$\frac{S}{N_a} = - \sum_{\sigma} \int [\eta_{\sigma} \ln(\eta_{\sigma}) + (1 - \eta_{\sigma}) \ln(1 - \eta_{\sigma})] \rho(\varepsilon) d\varepsilon. \quad (42)$$

Finally, knowing S , the interaction energy W is calculated from Eq. (29). For the moment we restrict ourselves to paramagnetic systems having the same electron density $n_{\sigma} = N_{\sigma}/N_a = \frac{1}{2}$ for both spins. In this case, we have $W_{\text{HF}} = U N_a/4$, $S_{\infty} = 2N_a \ln(2)$, and thus $\vartheta = U/(8 \ln 2)$. Spin-polarized systems will be considered in the following subsection.

In Fig. 5, results are given for the ground-state kinetic, Coulomb, and total energies of the half-filled Hubbard model in bipartite lattices having $d = 1-3$ dimensions, as well as in the limit $d \rightarrow \infty$. In the 1D case, we observe that IFE results for E_0 are nearly indistinguishable from the exact Bethe-ansatz solution [43]. The relative error $|E_0^{\text{ex}} - E_0^{\text{IFE}}|/|E_0^{\text{ex}}|$, shown in the inset of Fig. 5(c), is always smaller than 0.1%. In particular, the exact result $E_0 = -4N_a \ln(2) t^2/U$ is recovered in the strongly correlated Heisenberg limit. This is most remarkable since there are no adjustable parameters behind the IFE approximation but simply the linear ansatz relating W and S . Notice, moreover, that such a high accuracy is obtained despite the fact that the occupation numbers $\eta_{k\sigma}$ do not exhibit the expected Luttinger-liquid behavior [74]. This would require that the derivative of $\eta_{\sigma}(\varepsilon)$ diverges at $\varepsilon = \varepsilon_F$, which is of course not possible with a Fermi distribution [see Eq. (38)]. Most likely the precise behavior at ε_F , although crucial for the excitations and the temperature dependence, has little influence on the total energy of the system.

It is interesting to observe that the very good accuracy of the IFE approximation concerning the ground-state energy is not the result of a significant compensation of errors. Indeed, also the more difficult kinetic and double-occupation contributions to the ground-state energy are nearly indistinguishable from the exact solution for all values of U/t . This is clearly shown by comparing the blue crosses and solid curves in Fig. 5, as well as by the small relative errors, which are highlighted in the inset of Fig. 5(c). For example, the largest relative error in D ($\Delta D = 0.18\%$) is quite small, only slightly more important than the largest relative error in E ($\Delta E = 0.10\%$).

In 2D no exact solution of the half-filled Hubbard model is available. In the strongly correlated limit, one may infer E_0 from the ground-state energy $\varepsilon_{2\text{DH}}$ of the spin- $\frac{1}{2}$ Heisenberg model having an exchange constant $J = 1$. Performing the appropriate Schrieffer-Wolff transformation [75] for $U/t \gg 1$ one obtains $E_0 = -\alpha t^2/U$ with $\alpha = 2 - 4\varepsilon_{2\text{DH}}$ in the two-dimensional case. Taking $\varepsilon_{2\text{DH}} = -0.669$ from accurate quantum Monte Carlo (QMC) simulations on finite 2D square-lattice Heisenberg clusters with periodic boundary conditions [79] one finds for the Hubbard model $\alpha_{\text{QMC}} = 4.68$, while the IFE approximation yields $\alpha_{\text{IFE}} = 8 \ln 2 \approx 5.55$. Although the right dependence on t^2/U is obtained, the binding energy is overestimated by 18% in the strongly correlated limit. For finite values of U/t , our results for the 2D square lattice are in very good agreement with the far more demanding quantum Monte Carlo simulations reported in Refs. [76–78]. This applies both to the ground-state energy E [Fig. 5(a)] and

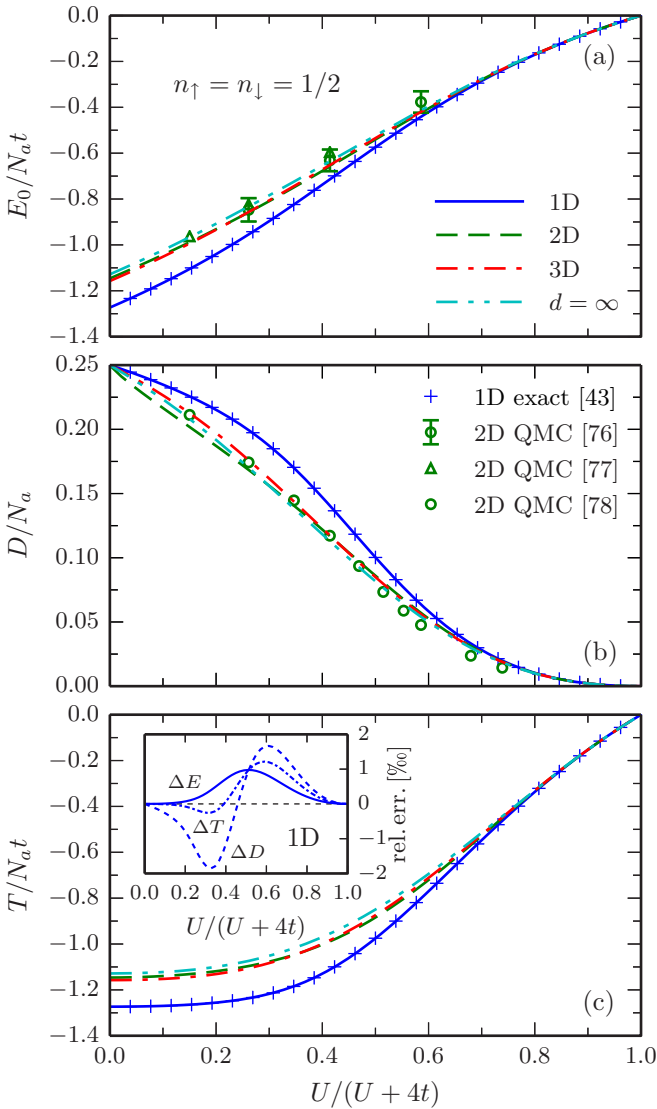


FIG. 5. Ground-state properties of the half-filled Hubbard model on hypercubic lattices having $d = 1-3$ dimensions and $d \rightarrow \infty$ as functions of the Coulomb-repulsion strength U/t . Results are given for the (a) ground-state energy E_0 , (b) average number of double occupations D , and (c) kinetic energy T . The curves were obtained in the linear independent-fermion entropy (IFE) approximation to LDFT. The symbols correspond either to the exact Bethe-ansatz solution [43] (crosses, 1D) or to numerical quantum Monte Carlo simulations [76–78] (open circles and triangles, 2D). For each dimension d the NN hopping integral t_d is scaled as $t_d = t/\sqrt{d}$ in order that the second moment of the local density of states $w_2 = 2dt_d^2$ is independent of d . The inset in (c) shows the relative difference $\Delta X = |X^{\text{ex}} - X^{\text{IFE}}|/|X^{\text{ex}}|$ where X stands for the total energy E_0 , the kinetic energy T , and the average double occupations D in the 1D case.

to the average number of double occupations D [Fig. 5(b)]. Compare the dashed green curves with the open circles and triangles. As in the 1D case, our approximation tends to underestimate D somewhat for weak to intermediate interaction strength ($U/t \lesssim 4$) and to overestimate it slightly for strong interactions ($U/t \gtrsim 4$). One concludes that in 2D not only the ground-state energy, but also more subtle observables such

as the average number of double occupations, are accurately obtained.

Concerning the dependence on the lattice dimension we find a surprisingly fast convergence to the limit of infinite dimensions, once the NN hoppings are scaled as $t_d = t/\sqrt{d}$ in order to yield the same second moment or variance $w_2 = 2dt_d^2 = 2t^2$ of the local DOS. This concerns not only the total energy, but also the kinetic and Coulomb contributions. One concludes that for $d \geq 2$, and in this approximation, most of the dependence of E_0 , T , and W on dimensionality is concealed in the variance of the single-particle spectrum. Notice that for a fixed NN hopping integral, the mean-root-square deviation $\sqrt{w_2}$ of the local DOS is proportional to \sqrt{d} , in contrast to the bandwidth w_b which is proportional to d . Therefore, the latter would not be the appropriate scaling measure. A further interesting result is the universal behavior found in the limit of strong correlations, i.e., for $U/w_2 > 4$ or equivalently $J = 4t_d^2/U < 1/2d$. In this Heisenberg limit ($U/t \gg 1$), the IFE approximation yields $E_0 = -Jd \ln(2) = -4d \ln(2)t_d^2/U$, which after the d -dependent scaling of the NN hopping becomes $E_0 = -4 \ln(2)t^2/U$ for all d . Quantum Monte Carlo simulations and exact diagonalizations on finite square-lattice clusters show that no such a simple scaling holds between the ground-state energies of the 1D and 2D Heisenberg models [79–81]. After proper scaling of the hopping integrals t_d the exact ratio between the 1D and 2D ground-state energies for $U/t \gg 1$ is $E_0^{1D}/E_0^{2D} = 1.185$ instead of 1 as predicted by the IFE approximation. This suggests that the convergence to the limit of infinite dimensions is probably slower than the one predicted in this work.

Once the occupation numbers $\eta_{k\sigma}$ which minimize the energy functional are obtained, it is straightforward to determine the density-matrix elements $\gamma_{ij\sigma}$ by Fourier transformation. In Fig. 6, results are given for $\gamma_{0\delta\sigma}$ between an atom $i = 0$ and its δ th-nearest neighbor in the half-filled 1D Hubbard model ($n_\uparrow = n_\downarrow = 1/2$). In Fig. 6(a), $\gamma_{0\delta\sigma}$ is shown as a function of U/t for different odd δ . For even δ one finds $\gamma_{0\delta\sigma} = 0$ due to electron-hole symmetry. As expected, $\gamma_{0\delta\sigma}$ decreases with increasing U/t since charge fluctuations are suppressed in order to reduce the average number of double occupations. Notice that the long-range fluctuations (larger δ) get suppressed faster than the short-range fluctuations. In particular, the $\gamma_{01\sigma}$ between NNs decreases very slowly, proportional to t/U in the limit $U/t \rightarrow \infty$, so that the kinetic energy $T \propto t^2/U$ remains finite for all finite U .

A different perspective is adopted in Fig. 6(b), where $\gamma_{0\delta\sigma}$ is plotted as a function of δ for representative values of U/t . One observes that $\gamma_{0\delta\sigma}$ decreases with increasing distance and with increasing U/t . Notice the oscillations and changes of sign in $\gamma_{0\delta\sigma}$ as a function of δ , which are particularly clear for small U/t and tend to be flattened as the interaction strength increases.

It is interesting to take advantage of the universality of LDFT and to consider lattice structures which may show different types of correlations, for example, as a result of magnetic frustrations. The IFE approximation to the interaction-energy functional W has been applied to the half-filled Hubbard model on the 2D triangular lattice in order to explore this problem. The results obtained for the ground-state energy, kinetic energy, and average number of double occupations are presented in Fig. 7.

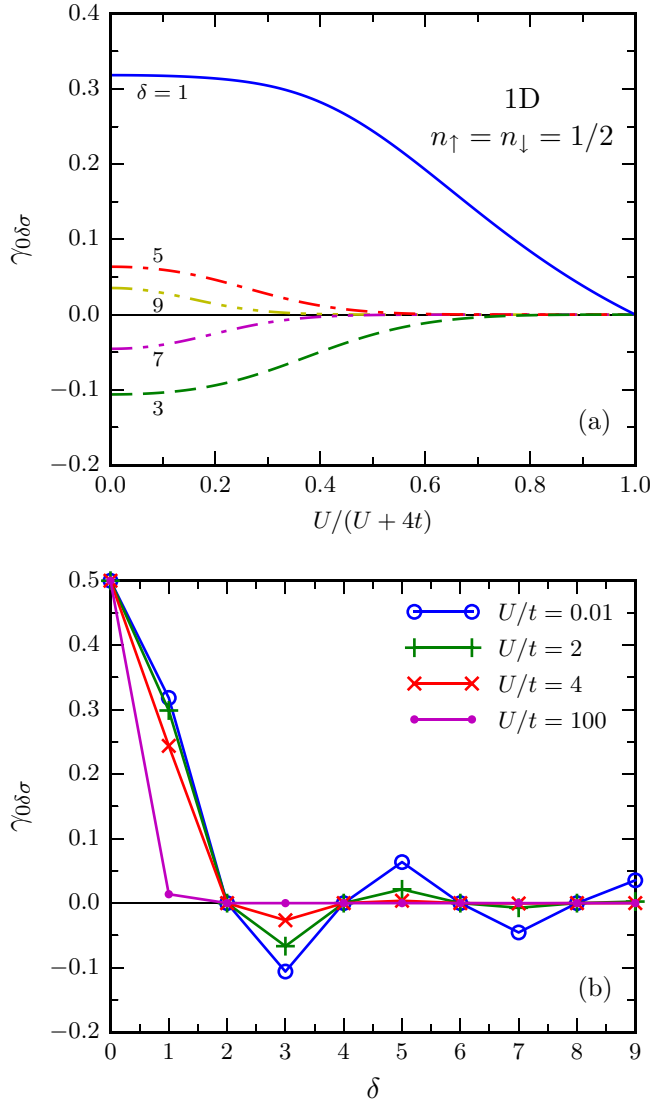


FIG. 6. Single-particle density-matrix elements $\gamma_{0\delta\uparrow} = \gamma_{0\delta\downarrow}$ between an atom $i = 0$ and its δ th-nearest neighbor in the ground state of the half-filled 1D Hubbard model, as obtained by using the linear IFE approximation. In (a), $\gamma_{0\delta\sigma}$ is given for odd δ as a function of the Coulomb-repulsion strength U/t . Electron-hole symmetry implies $\gamma_{0\delta\sigma} = 0$ for even δ . In (b), $\gamma_{0\delta\sigma}$ is shown as a function of δ for representative values of U/t .

One observes that the dependence on U/t is qualitatively similar to the one derived from exact diagonalizations on a finite 4×4 cluster with periodic boundary conditions. In the weakly correlated limit, the IFE approximation recovers the Hartree-Fock average number of double occupations $D_{\text{HF}} = \frac{1}{4}$. In contrast to previous finite-system calculations, no limitations resulting from degeneracies in the single-particle spectrum are present. On the other side, in the strongly correlated limit one obtains $E_0/N_a \simeq -\alpha t^2/U$ with $\alpha_{\text{IFE}} = 8.62$. This can be compared with numerical estimates based on exact diagonalizations of the 2D triangular Heisenberg model, from which one infers $\alpha = 7.41$ [82]. The corresponding relative error is thus only about 16%, which is significantly smaller than in the previously discussed case of finite triangular lattices.

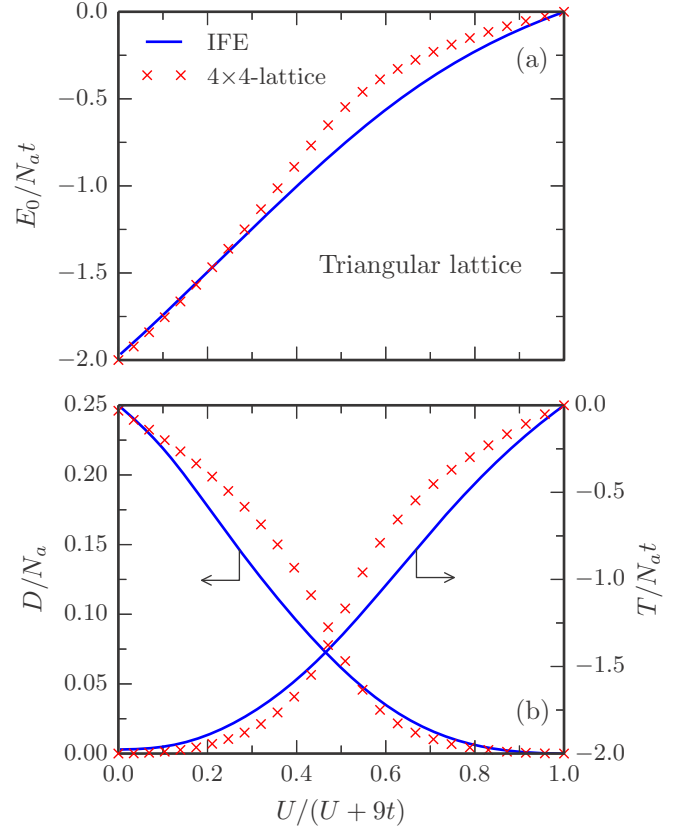


FIG. 7. Ground-state properties of the half-filled Hubbard model on the infinite 2D triangular lattice: (a) total energy E_0 and (b) average number of double occupations D and kinetic energy T , as functions of the Coulomb-repulsion strength U/t . The full curves are obtained by using the linear independent-fermion entropy (IFE) approximation to LDFT, while the crosses correspond to the exact diagonalization of a finite 4×4 plaquette with periodic boundary conditions.

D. Spin-polarized systems

In order to investigate the dependence on the spin polarization, we minimize the energy functional $E[\eta_{k\sigma}]$ under the constraint of fixed $n_{\uparrow} - n_{\downarrow} = 2S_z/N_a$. Figure 8 shows the IFE results for the ground-state total, kinetic and Coulomb energies of the half-filled 1D Hubbard model as a function of S_z . As expected, $S_z = 0$ always yields the minimum E , since at half-band filling the ground state has a total spin $S = 0$ for all U/t [43]. The energy change $\Delta E = E(S_z) - E(0)$ with increasing $|S_z|$ is the result of the interplay between the kinetic-energy increase and the Coulomb-energy decrease as the occupations $\eta_{k\sigma}$ of the antibonding majority-spin Bloch states (e.g., $\varepsilon_{k\uparrow} > 0$) grow at the expense of the occupations of bonding minority-spin states (e.g., $\varepsilon_{k\downarrow} < 0$) [see Figs. 8(b) and 8(c)]. With increasing $|S_z|$ double occupations are progressively suppressed since the probability of finding a pair of electrons with opposite spins at the same site decreases. In the fully polarized state (i.e., for $|S_z| = N_a/2$) all lattice sites have one majority-spin electron and therefore local charge fluctuations are completely suppressed. This implies vanishing T , D , and E for all U/t [see Figs. 8(b) and 8(c)]. Since E is a monotonic increasing function of U/t , in particular for $S_z = 0$, it is clear that the largest energy change $\Delta E(S_z = N_a/2)$ must

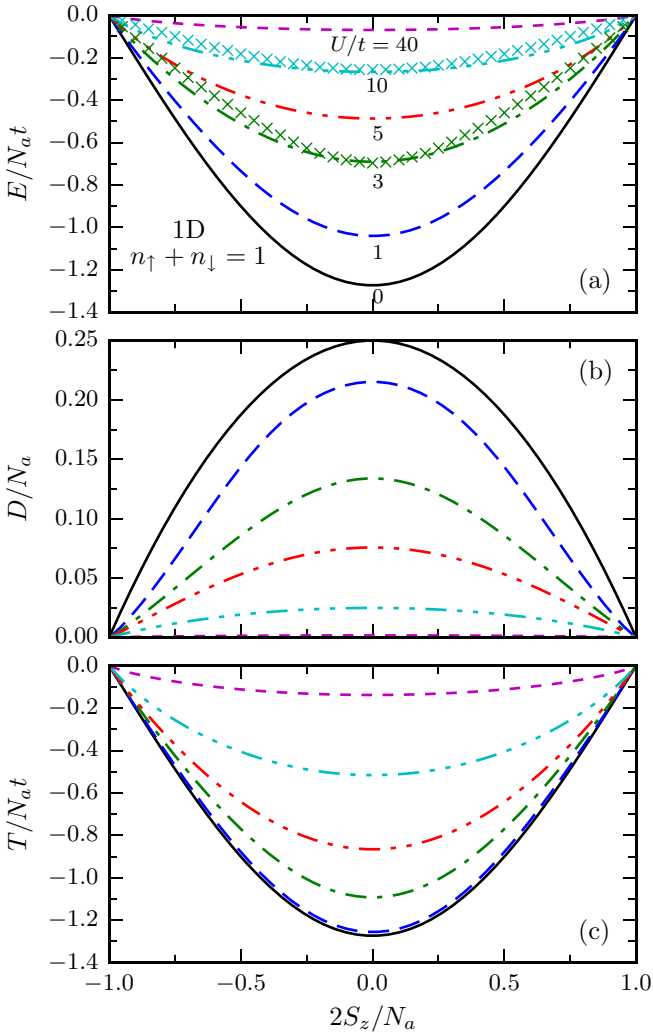


FIG. 8. Ground-state properties of the one-dimensional half-filled Hubbard model as functions of the spin polarization per atom $n_\uparrow - n_\downarrow = 2S_z/N_a$ for representative Coulomb-repulsion strengths U/t : (a) total energy E , (b) average number of double occupations D , and (c) kinetic energy T . The curves were obtained using the IFE approximation to LDFT, while the crosses in (a) for $U/t = 3$ and 10 are results taken from Ref. [83].

decrease with increasing U/t reaching $\Delta E = 0$ for all S_z when $U/t = \infty$. In other words, the energy of the system tends to become independent of the total spin S in the strongly correlated limit, as the effective Heisenberg exchange-coupling constant $J = 4t^2/U$ between the localized spins tends to zero.

The precise form of $\Delta E(S_z)$ depends on the Coulomb-repulsion strength U/t , which measures the relative importance between T and W , and on the shape of the single-particle local density of states $\rho_\sigma(\varepsilon)$, which is different for different lattices. For small S_z it can be written as

$$\frac{\Delta E}{N_a} = \frac{\mu^2 N_a}{2\chi} \left(\frac{S_z}{N_a} \right)^2 + O(S_z^4), \quad (43)$$

where μ is the magnetic moment of the electron and χ stands for the zero-field susceptibility. For $U = 0$, χ takes the well-known Pauli value $\chi_P = \mu^2 N_a \rho(\varepsilon_F)/4$, which is proportional

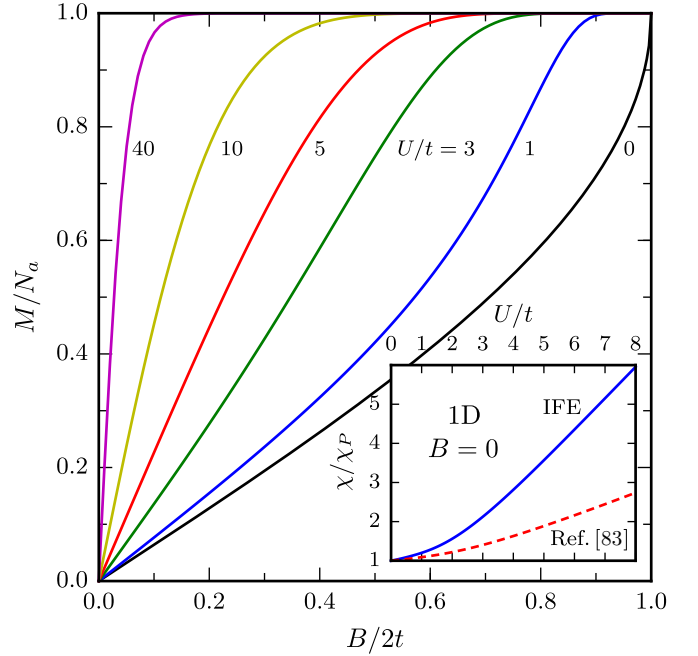


FIG. 9. Ground-state magnetization $M = 2S_z$ of the one-dimensional half-filled Hubbard model as a function of the applied magnetic field B , for different values of the Coulomb repulsion U , as obtained by using the IFE approximation. In the inset, the zero-field susceptibility is shown as a function of U/t , where χ_P stands for the Pauli susceptibility. The solid curve shows the present IFE approximation, while the dashed curve shows exact results from Ref. [83].

to the local DOS $\rho = \rho_\uparrow + \rho_\downarrow$ at the Fermi energy ε_F . In Fig. 8, the IFE results for $E(S_z)$ are compared with the development reported by Takahashi in Ref. [83], which is based on the exact Bethe-ansatz solution and which is exact in the limit of $S_z \rightarrow 0$. A quite satisfactory overall agreement between the two approaches is observed for the two available values of $U/t = 3$ and 10 . However, notice that the IFE approximation tends to systematically underestimate the curvature of $E(S_z)$ in the vicinity of $S_z = 0$. This anticipates an overestimation of the zero-field susceptibility χ , as it will be discussed below.

In order to calculate the ground-state magnetization $M = 2S_z$ induced by a uniform external magnetic field $\mathbf{B} = B\hat{e}_z$ and the zero-field susceptibility $\chi = \partial M/\partial B$, we use our previous results for $E(S_z)$ and simply minimize the ground-state energy $E_B = E(S_z) + \mu B S_z$ with respect to S_z . Figure 9 shows the results for the 1D half-filled Hubbard model. One observes, as expected, that M increases monotonously with increasing B until saturation is reached (i.e., $M/N_a = 1$). The spin polarization and in particular the slope χ at $B = 0$ are increasing functions of U/t . Thus, the field at which M reaches saturation decreases with increasing U/t (see Fig. 9). The more rapid increase of M as a function of B for stronger Coulomb repulsion can be understood by noting that the width $\Delta E(N_a/2)$ of the spin or Zeeman band decreases with increasing U/t (see Fig. 8). Moreover, from a quasiparticle perspective, it can be interpreted as an enhancement of the effective density of states at the Fermi energy, or equivalently

as an enhancement of the effective mass of the electrons, as U/t increases.

The zero-field susceptibility χ can be directly related to the curvature α of the ground-state energy E as a function of S_z at $S_z = 0$. From $\Delta E(S_z) = \alpha S_z^2 + O(S_z^4)$, one readily obtains $\chi = \mu^2/2\alpha$. In the inset of Fig. 9, the IFE calculations are compared with Takahashi's exact results for the half-filled 1D Hubbard model [83]. As expected, we recover the Pauli susceptibility $\chi = \chi_P$ for $U = 0$. We also qualitatively explain the increase of χ with increasing Coulomb-repulsion strength, as the electrons tend to localize and the spin band narrows. Finally, in the strongly correlated limit ($U/t \gg 1$), we obtain that χ increases linearly with U/t , in agreement with the exact solution. However, the IFE approximation yields $\chi \simeq (\pi \chi_P/4)(U/t)$, while the exact asymptotic behavior is given by $\chi \simeq (\chi_P/\pi)(U/t)$. Therefore, the IFE approximation seriously overestimates the strongly correlated magnetic susceptibility by a factor $\pi^2/4 \simeq 2.5$. This is consistent with the already mentioned underestimation of the curvature of $E(S_z)$ in the vicinity $S_z = 0$, which is shown in Fig. 8(a). It means that the approximation overestimates the density of many-body states having finite total spin $S > 0$ in the vicinity of $S = 0$.

V. SUMMARY AND OUTLOOK

The half-filled Hubbard model has been investigated in the framework of lattice density functional theory (LDFT). To this aim, the interaction energy of the model is regarded as a functional $W[\gamma_\sigma]$ of the single-particle density matrix γ_σ of spin σ . The periodicity of the lattice allows us to adopt a \mathbf{k} -space perspective. Thus, W can be expressed as a functional of the occupation numbers $\eta_{k\sigma}$ of the natural orbitals of γ_σ , which are Bloch states having a well-defined wave vector \mathbf{k} . By analyzing the limits of weak and strong correlations we were able to establish useful general links between $W[\eta_{k\sigma}]$ and the independent-fermion entropy $S[\eta_{k\sigma}]$ associated to the natural-orbital occupations $\eta_{k\sigma}$. Exact numerical results for W provide additional support to the statistical analogy by revealing the approximate relation between W and S . A simple explicit linear ansatz of the form $W = W(S[\eta_{k\sigma}])$ has been proposed, which is suitable for extensive applications. In order to obtain the ground-state properties, the energy functional $E = T + W$ is minimized with respect to $\eta_{k\sigma}$, where $T = \sum_{k\sigma} \eta_{k\sigma} \varepsilon_k$ stands for the kinetic energy functional. A Fermi-type distribution of the ground state $\eta_{k\sigma}$ is thus obtained, in which Hubbard's local Coulomb repulsion U plays the role of an effective temperature. The present \mathbf{k} -space formulation constitutes an important alternative to previous real-space approaches to LDFT.

A number of applications of the linear independent-fermion entropy (IFE) approximation have been performed for the Hubbard model on finite and infinite lattices having $d = 1-3$ dimensions as well as in the limit of $d \rightarrow \infty$. Comparison with exact results and state-of-the-art numerical simulations, which are available for one- and two-dimensional systems, shows a good agreement as a function of the Coulomb-repulsion strength U/t from weak to strong correlations. Remarkably accurate are the IFE results in 1D, where in particular the strongly correlated Heisenberg limit is exactly reproduced.

However, inaccuracies in the zero-field magnetic susceptibility χ are also observed in 1D for $U/t \rightarrow \infty$.

Concerning the trends for different lattice structures, one observes that the accuracy of the proposed approximation improves as the dimension or the coordination number of the system decreases. Thus, the 1D lattice is described more precisely than the 2D square lattice, which in turn is described more precisely than the triangular 2D lattice. Moreover, the accuracy improves with increasing system size both in the weakly and strongly correlated regimes, as illustrated, for example, by the calculations for finite and infinite triangular lattices. The statistical analogy underlying the IFE approach seems therefore more suitable for continuous single-particle spectra.

Two reasons probably contribute to the success of the present approximation to LDFT. First, in single-band periodic systems, the natural orbitals $u_{ik\sigma} = e^{-i\mathbf{k}\cdot\mathbf{R}_i}/\sqrt{N_a}$ are independent of U/t . Therefore, irrespectively of the system dimensions, the dependence of W on the shape of the natural orbitals need not be treated explicitly (translational symmetry). Second, the Fermi-type distribution of $\eta_{k\sigma}$ obtained in the IFE approximation is continuous, as the Luttinger-liquid distribution. This suggests that the IFE approximation should be best suited for the 1D case. As we move to 3D and Fermi-liquid behavior sets in, it is reasonable to expect that the accuracy should tend to worsen to some extent since the IFE approximation cannot reproduce a proper step in the occupation numbers. Nevertheless, the overall quality of the results justifies the validity of the independent-fermion entropy ansatz, thus shedding new light onto the complex functional dependence of $W[\gamma_\sigma]$ for weakly and strongly correlated systems.

The present investigations open a number of interesting perspectives for extensions and improvements. The applications performed in this work concern periodic systems, which allowed us to focus on the functional dependence of W on the occupation numbers $\eta_{k\sigma}$. The natural orbitals $u_{ik\sigma}$, being Bloch states, are independent of the interaction strength. While this certainly represents a major simplification, we also know that the translational invariance of the system is not a prerequisite for the basic links between interaction energy W and independent-fermion entropy S . Indeed, as discussed in Sec. III, even in the general case, we have that idempotent γ , which describes uncorrelated states having integer natural-orbital occupations, corresponds to a vanishing S , while scalar γ , which describes strongly correlated localized electrons, corresponds to maximal S . In order to describe systems showing nonuniform charge distributions, the dependence of W on the natural orbitals $u_{ik\sigma}$ has to be taken into account explicitly.

Another interesting related problem is to investigate the effects of an external magnetic field, for example, perpendicular to the 2D square lattice. This introduces Peierls phases in the NN hopping integrals, depending on the flux enclosed by the unit cell [84,85] which often lead to remarkable topological effects. Such applications would require more complicated minimization procedures of the total-energy functional, for example, as proposed in Ref. [69]. Exploring strongly correlated systems in which the shape of the natural orbitals depends on U/t should help us understand if the simple IFE approximation

remains an accurate ansatz or if it should be regarded as the limit of more sophisticated approaches.

A further challenge is to vary the band filling and thereby quantify the stability of ferromagnetic ground states. In the half-filled-band case considered so far, the only way of achieving a vanishing interaction energy W is that γ becomes scalar, i.e., $\gamma_{ij\sigma} = 0$ for $i \neq j$ or $\eta_{k\sigma} = N_{\sigma}/N_a$ for all \mathbf{k} . This corresponds to localized many-electron states having zero kinetic energy T and total energy E . This allowed us to safely associate strong correlations to maximum single-particle entropy. However, it is well known that away from half-band filling there are states which have a vanishing interaction energy $W = 0$ and at the same time a finite kinetic energy $T < 0$. The fully polarized ferromagnetic state is one but not the only example [59]. Therefore, in order to go beyond half-band filling with the present approach, it would be necessary to extend the functional $W[\eta_{k\sigma}]$ in order to allow for \mathbf{k} -dependent occupation-number distributions $\eta_{k\sigma}$ in the strongly correlated limit.

Finally, we would like to draw your attention to the energy dependence of the Bloch-state occupation $\eta_{k\sigma}$ near the Fermi energy. In this work, we have shown that for *any* independent-fermion entropy ansatz of the form $W = W(S)$, the ground state $\eta_{k\sigma}$ follows a Fermi distribution as a function of the single-particle energy ε_k , which of course depends on the interaction strength. Such a smooth nonsingular energy dependence at ε_F allows us to describe neither the Luttinger-liquid behavior expected in 1D nor the Fermi-liquid behavior appropriate to 3D. Although this limitation happens to have little consequences on the average ground-state properties, the situation is likely to be different when looking at low-energy excitations, temperature effects, or transport properties, which are most sensitive to the quasiparticle states at ε_F . It would be therefore very interesting to consider more general approaches to $W[\eta_{k\sigma}]$, beyond the IFE ansatz, in order to identify under which circumstances Luttinger or Fermi behaviors appear in LDFT, particularly in connection with the dimensionality and topology of the lattice.

-
- [1] P. Hohenberg and W. Kohn, Inhomogeneous electron gas, *Phys. Rev.* **136**, B864 (1964).
- [2] W. Kohn and L. J. Sham, Self-consistent equations including exchange and correlation effects, *Phys. Rev.* **140**, A1133 (1965).
- [3] U. von Barth and L. Hedin, A local exchange-correlation potential for the spin polarized case: I, *J. Phys. C: Solid State Phys.* **5**, 1629 (1972).
- [4] D. C. Langreth and M. J. Mehl, Beyond the local-density approximation in calculations of ground-state electronic properties, *Phys. Rev. B* **28**, 1809 (1983).
- [5] A. D. Becke, Density-functional exchange-energy approximation with correct asymptotic behavior, *Phys. Rev. A* **38**, 3098 (1988).
- [6] J. P. Perdew, K. Burke, and M. Ernzerhof, Generalized Gradient Approximation Made Simple, *Phys. Rev. Lett.* **77**, 3865 (1996).
- [7] J. Toulouse, I. C. Gerber, G. Jansen, A. Savin, and J. G. Ángyán, Adiabatic-Connection Fluctuation-Dissipation Density-Functional Theory Based on Range Separation, *Phys. Rev. Lett.* **102**, 096404 (2009).
- [8] J. Toulouse, W. Zhu, J. G. Ángyán, and A. Savin, Range-separated density-functional theory with the random-phase approximation: Detailed formalism and illustrative applications, *Phys. Rev. A* **82**, 032502 (2010).
- [9] W. Zhu, J. Toulouse, A. Savin, and J. G. Ángyán, Range-separated density-functional theory with random phase approximation applied to noncovalent intermolecular interactions, *J. Chem. Phys.* **132**, 244108 (2010).
- [10] T. L. Gilbert, Hohenberg-Kohn theorem for nonlocal external potentials, *Phys. Rev. B* **12**, 2111 (1975).
- [11] A. M. K. Müller, Explicit approximate relation between reduced two- and one-particle density matrices, *Phys. Lett. A* **105**, 446 (1984).
- [12] S. Goedecker and C. J. Umrigar, Natural Orbital Functional for the Many-Electron Problem, *Phys. Rev. Lett.* **81**, 866 (1998).
- [13] E. J. Baerends, Exact Exchange-Correlation Treatment of Dissociated H_2 in Density Functional Theory, *Phys. Rev. Lett.* **87**, 133004 (2001).
- [14] M. A. Buijse and E. J. Baerends, An approximate exchange-correlation hole density as a functional of the natural orbitals, *Mol. Phys.* **100**, 401 (2002).
- [15] O. Gritsenko, K. Pernal, and E. J. Baerends, An improved density matrix functional by physically motivated repulsive corrections, *J. Chem. Phys.* **122**, 204102 (2005).
- [16] D. R. Rohr, K. Pernal, O. V. Gritsenko, and E. J. Baerends, A density matrix functional with occupation number driven treatment of dynamical and nondynamical correlation, *J. Chem. Phys.* **129**, 164105 (2008).
- [17] M. Piris, A new approach for the two-electron cumulant in natural orbital functional theory, *Int. J. Quantum Chem.* **106**, 1093 (2006).
- [18] M. Piris, X. Lopez, F. Ruipérez, J. M. Matxain, and J. M. Ugalde, A natural orbital functional for multiconfigurational states, *J. Chem. Phys.* **134**, 164102 (2011).
- [19] M. A. L. Marques and N. N. Lathiotakis, Empirical functionals for reduced-density-matrix-functional theory, *Phys. Rev. A* **77**, 032509 (2008).
- [20] N. N. Lathiotakis and M. A. L. Marques, Benchmark calculations for reduced density-matrix functional theory, *J. Chem. Phys.* **128**, 184103 (2008).
- [21] N. N. Lathiotakis, S. Sharma, J. K. Dewhurst, F. G. Eich, M. A. L. Marques, and E. K. U. Gross, Density-matrix-power functional: Performance for finite systems and the homogeneous electron gas, *Phys. Rev. A* **79**, 040501 (2009).
- [22] D. R. Rohr, J. Toulouse, and K. Pernal, Combining density-functional theory and density-matrix-functional theory, *Phys. Rev. A* **82**, 052502 (2010).
- [23] W. Heitler and F. London, Wechselwirkung neutraler Atome und homöopolare Bindung nach der Quantenmechanik, *Z. Phys.* **44**, 455 (1927).
- [24] A. C. Hewson, *The Kondo Problem to Heavy Fermions* (Cambridge University Press, Cambridge, UK, 1993).
- [25] G. D. Mahan, *Many-Particle Physics*, 3rd ed., Physics of Solids and Liquids (Springer, New York, 2000).
- [26] E. Dagotto, Correlated electrons in high-temperature superconductors, *Rev. Mod. Phys.* **66**, 763 (1994).

- [27] A. Georges, G. Kotliar, W. Krauth, and M. J. Rozenberg, Dynamical mean-field theory of strongly correlated fermion systems and the limit of infinite dimensions, *Rev. Mod. Phys.* **68**, 13 (1996).
- [28] M. Imada, A. Fujimori, and Y. Tokura, Metal-insulator transitions, *Rev. Mod. Phys.* **70**, 1039 (1998).
- [29] K. N. Kudin, G. E. Scuseria, and R. L. Martin, Hybrid Density-Functional Theory and the Insulating Gap of UO_2 , *Phys. Rev. Lett.* **89**, 266402 (2002).
- [30] I. D. Prodan, G. E. Scuseria, and R. L. Martin, Assessment of metageneralized gradient approximation and screened Coulomb hybrid density functionals on bulk actinide oxides, *Phys. Rev. B* **73**, 045104 (2006).
- [31] I. D. Prodan, G. E. Scuseria, and R. L. Martin, Covalency in the actinide dioxides: Systematic study of the electronic properties using screened hybrid density functional theory, *Phys. Rev. B* **76**, 033101 (2007).
- [32] X.-D. Wen, R. L. Martin, L. E. Roy, G. E. Scuseria, S. P. Rudin, E. R. Batista, T. M. McCleskey, B. L. Scott, E. Bauer, J. J. Joyce, and T. Durakiewicz, Effect of spin-orbit coupling on the actinide dioxides $An\text{O}_2$ ($An = \text{Th}, \text{Pa}, \text{U}, \text{Np}, \text{Pu}, \text{and Am}$): A screened hybrid density functional study, *J. Chem. Phys.* **137**, 154707 (2012).
- [33] V. Eyert, VO_2 : A Novel View from Band Theory, *Phys. Rev. Lett.* **107**, 016401 (2011).
- [34] F. Iori, M. Gatti, and A. Rubio, Role of nonlocal exchange in the electronic structure of correlated oxides, *Phys. Rev. B* **85**, 115129 (2012).
- [35] R. Pariser and R. G. Parr, A Semi-Empirical Theory of the Electronic Spectra and Electronic Structure of Complex Unsaturated Molecules. I. *J. Chem. Phys.* **21**, 466 (1953).
- [36] J. A. Pople, Electron interaction in unsaturated hydrocarbons, *Trans. Faraday Soc.* **49**, 1375 (1953).
- [37] P. W. Anderson, Localized magnetic states in metals, *Phys. Rev.* **124**, 41 (1961).
- [38] J. Hubbard, Electron Correlations in Narrow Energy Bands, *Proc. R. Soc. London A* **276**, 238 (1963).
- [39] J. Kanamori, Electron Correlation and Ferromagnetism of Transition Metals, *Prog. Theor. Phys.* **30**, 275 (1963).
- [40] M. C. Gutzwiller, Effect of Correlation on the Ferromagnetism of Transition Metals, *Phys. Rev. Lett.* **10**, 159 (1963).
- [41] P. Fulde, *Electron Correlations in Molecules and Solids*, 3rd ed., Springer Series in Solid-state Sciences No. 100 (Springer, Berlin, 1995).
- [42] N. H. March, *Electron Correlation in Molecules and Condensed Phases* (Springer, New York, 1996).
- [43] E. H. Lieb and F. Y. Wu, Absence of Mott Transition in an Exact Solution of the Short-Range, One-Band Model in One Dimension, *Phys. Rev. Lett.* **20**, 1445 (1968).
- [44] H. Shiba, Magnetic Susceptibility at Zero Temperature for the One-Dimensional Hubbard Model, *Phys. Rev. B* **6**, 930 (1972).
- [45] Y. Nagaoka, Ground state of correlated electrons in a narrow almost half-filled s band, *Solid State Commun.* **3**, 409 (1965).
- [46] H. Tasaki, Extension of nagaoka's theorem on the large- U hubbard model, *Phys. Rev. B* **40**, 9192 (1989).
- [47] E. H. Lieb, Two Theorems on the Hubbard Model, *Phys. Rev. Lett.* **62**, 1927 (1989).
- [48] S. R. White, D. J. Scalapino, R. L. Sugar, E. Y. Loh, J. E. Gubernatis, and R. T. Scalettar, Numerical study of the two-dimensional Hubbard model, *Phys. Rev. B* **40**, 506 (1989).
- [49] N. Furukawa and M. Imada, Charge Gap, Charge Susceptibility and Spin Correlation in the Hubbard Model on a Square Lattice, *J. Phys. Soc. Jpn.* **60**, 3604 (1991).
- [50] S. R. White, Density Matrix Formulation for Quantum Renormalization Groups, *Phys. Rev. Lett.* **69**, 2863 (1992).
- [51] S. R. White, Density-matrix algorithms for quantum renormalization groups, *Phys. Rev. B* **48**, 10345 (1993).
- [52] O. Gunnarsson and K. Schönhammer, Density-Functional Treatment of an Exactly Solvable Semiconductor Model, *Phys. Rev. Lett.* **56**, 1968 (1986).
- [53] A. Svane and O. Gunnarsson, Localization in the self-interaction-corrected density-functional formalism, *Phys. Rev. B* **37**, 9919 (1988).
- [54] K. Schönhammer, O. Gunnarsson, and R. M. Noack, Density-functional theory on a lattice: Comparison with exact numerical results for a model with strongly correlated electrons, *Phys. Rev. B* **52**, 2504 (1995).
- [55] A. Schindlmayr and R. W. Godby, Density-functional theory and the v -representability problem for model strongly correlated electron systems, *Phys. Rev. B* **51**, 10427 (1995).
- [56] A. E. Carlsson, Exchange-correlation functional based on the density matrix, *Phys. Rev. B* **56**, 12058 (1997).
- [57] N. A. Lima, M. F. Silva, L. N. Oliveira, and K. Capelle, Density Functionals Not Based on the Electron Gas: Local-Density Approximation for a Luttinger Liquid, *Phys. Rev. Lett.* **90**, 146402 (2003).
- [58] C. Verdozzi, Time-Dependent Density-Functional Theory and Strongly Correlated Systems, *Phys. Rev. Lett.* **101**, 166401 (2008).
- [59] R. López-Sandoval and G. M. Pastor, Density-matrix functional theory of the Hubbard model: An exact numerical study, *Phys. Rev. B* **61**, 1764 (2000).
- [60] R. López-Sandoval and G. M. Pastor, Density-matrix functional theory of strongly correlated lattice fermions, *Phys. Rev. B* **66**, 155118 (2002).
- [61] R. López-Sandoval and G. M. Pastor, Electronic properties of the dimerized one-dimensional Hubbard model using lattice density-functional theory, *Phys. Rev. B* **67**, 035115 (2003).
- [62] R. López-Sandoval and G. M. Pastor, Interaction-energy functional for lattice density functional theory: Applications to one-, two-, and three-dimensional Hubbard models, *Phys. Rev. B* **69**, 085101 (2004).
- [63] W. Töws and G. M. Pastor, Lattice density functional theory of the single-impurity Anderson model: Development and applications, *Phys. Rev. B* **83**, 235101 (2011).
- [64] W. Töws and G. M. Pastor, Spin-polarized density-matrix functional theory of the single-impurity Anderson model, *Phys. Rev. B* **86**, 245123 (2012).
- [65] W. Töws, M. Saubanère, and G. M. Pastor, Density-matrix functional theory of strongly correlated fermions on lattice models and minimal-basis Hamiltonians, *Theor. Chem. Acc.* **133**, 1 (2014).
- [66] M. Saubanère and G. M. Pastor, Scaling and transferability of the interaction-energy functional of the inhomogeneous Hubbard model, *Phys. Rev. B* **79**, 235101 (2009).
- [67] M. Saubanère and G. M. Pastor, Density-matrix functional study of the Hubbard model on one- and two-dimensional bipartite lattices, *Phys. Rev. B* **84**, 035111 (2011).

- [68] M. Saubanère and G. M. Pastor, Lattice density-functional theory of the attractive Hubbard model, *Phys. Rev. B* **90**, 125128 (2014).
- [69] M. Saubanère, M. B. Lepetit, and G. M. Pastor, Interaction-energy functional of the Hubbard model: Local formulation and application to low-dimensional lattices, *Phys. Rev. B* **94**, 045102 (2016).
- [70] M. Levy, Universal variational functionals of electron densities, first-order density matrices, and natural spin-orbitals and solution of the v -representability problem, *Proc. Natl. Acad. Sci. USA* **76**, 6062 (1979).
- [71] L. D. Landau and E. M. Lifshitz, *Statistical Physics*, 3rd ed., Course of Theoretical Physics, Vol. 5 (Pergamon, New York, 1980), p. 160 ff.
- [72] C. Lanczos, An iteration method for the solution of the eigenvalue problem of linear differential and integral operators, *J. Res. Natl. Bur. Stand.* **45**, 255 (1950).
- [73] B. N. Parlett, *The Symmetric Eigenvalue Problem* (SIAM, Philadelphia, 1998).
- [74] F. H. L. Essler, H. Frahm, F. Göhmann, A. Klümper, and V. E. Korepin, *The One-Dimensional Hubbard Model* (Cambridge University Press, Cambridge, 2005).
- [75] J. R. Schrieffer and P. A. Wolff, Relation between the anderson and kondo Hamiltonians, *Phys. Rev.* **149**, 491 (1966).
- [76] J. E. Hirsch, Monte Carlo Study of the Two-Dimensional Hubbard Model, *Phys. Rev. Lett.* **51**, 1900 (1983).
- [77] A. Moreo, D. J. Scalapino, R. L. Sugar, S. R. White, and N. E. Bickers, Numerical Study of the Two-Dimensional Hubbard Model for Various Band Fillings, *Phys. Rev. B* **41**, 2313 (1990).
- [78] C. N. Varney, C.-R. Lee, Z. J. Bai, S. Chiesa, M. Jarrell, and R. T. Scalettar, Quantum Monte Carlo study of the two-dimensional fermion Hubbard model, *Phys. Rev. B* **80**, 075116 (2009).
- [79] M. C. Buonaura and S. Sorella, Numerical study of the two-dimensional heisenberg model using a green function monte carlo technique with a fixed number of walkers, *Phys. Rev. B* **57**, 11446 (1998).
- [80] L. Hulthén, Über das Austauschproblem eines Kristalls, *Ark. Mat. Astron. Fys.* **26A**, 11 (1938).
- [81] D. C. Mattis and C. Y. Pan, Ground-State Energy of Heisenberg Antiferromagnet for Spins $s = \frac{1}{2}$ and $s = 1$ in $d = 1$ and 2 Dimensions, *Phys. Rev. Lett.* **61**, 463 (1988).
- [82] S. Fujiki, Zero-Temperature Properties of Quantum Spin Models on the Triangular Lattice III: The Heisenberg Antiferromagnet, *Can. J. Phys.* **65**, 489 (1987).
- [83] M. Takahashi, Magnetization Curve for the Half-Filled Hubbard Model, *Prog. Theor. Phys.* **42**, 1098 (1969); Magnetic Susceptibility for the Half-Filled Hubbard Model, **43**, 1619 (1970).
- [84] R. E. Peierls, On the Theory of Diamagnetism of Conduction Electrons, *Z. Phys.* **80**, 763 (1933).
- [85] E. Brown, Bloch electrons in a uniform magnetic field, *Phys. Rev.* **133**, A1038 (1964).